

ALMA MATER STUDIORUM – UNIVERSITÀ DI BOLOGNA
DIPARTIMENTO DI INGEGNERIA CIVILE, CHIMICA, AMBIENTALE E DEI
MATERIALI

Civil Engineering Master Degree

Tesi di Laurea
in
Engineering Geology

***Structural health of a road tunnel intersecting a
large and active rockslide***

CANDIDATE:

Pietro Festi

SUPERVISOR:

Lisa Borgatti

COSUPERVISORS:

Alessandro Marzani

Gianluca Marcato

Giulia Bossi

Mirko Francioni

Chiara Staboli

Academic year 2021/22

IV Graduation Session

• ***Intentionally blank page*** •

Index

Introduction	4
San Lorenzo Tunnel	6
<i>General outlook</i>	6
<i>Geographic site</i>	8
<i>Geologic and geomorphologic setting</i>	10
<i>Climate</i>	12
<i>Hydrology</i>	12
<i>Passo della Morte landslide</i>	14
<i>State of art</i>	15
<i>Monitoring system</i>	18
Analysis and Modeling: methods	19
<i>Mesh creation through Photogrammetry</i>	20
<i>Mesh georeferencing</i>	36
<i>Cracks pattern mapping</i>	39
<i>FEM model elaboration</i>	42
Conclusions	62
References	75

Introduction

This work presents the case of the San Lorenzo road tunnel, a transportation infrastructure located in Friuli Venezia Giulia, in the northern part of Italy, involved in the so-called Passo della Morte landslide.

The area of the Carnic Alps, where the road tunnel of interest is inserted, has been remarkably famous for slope instability phenomena, mostly related to its geographical and geomorphological setting. In particular, the tunnel crosses a large rockslide of about 27 million m³ of material over an extension of 450 thousand m², characterized by slow movements settling around 2-3 cm/year. The delicate overall equilibrium condition of the slopes surrounding the road tunnel, already compromised by the many more landslide phenomena detected in the area, has been further threatened by the implementation of the road infrastructure itself, which has, indeed, encountered several problems since the beginning of the construction works. Damages like considerable water seepage inside the tunnel and concrete lining detachments have surfaced through the years, increasing the risk for the safety of the users of the road.

The first section of this work aims to give the proper amount of information about the global framework, required to be able to dig into this complex case of interest. Hence, a description of the main characteristics and features of both the landslide and the infrastructure will help in understand the huge number of aspects that needs to be considered when dealing with this case. In particular, the needed information about site geography and its strategic relevance, geological setting, hydrological and climate conditions will be provided, and eventually the road tunnel infrastructure itself, its interaction with the landslide phenomena and its current condition will be discussed.

A relevant mention will be given also to the monitoring system composed by crackmeters, clinometers, inclinometers and piezometers, which has been working for more than 20 years and has been developed to control the ongoing situation and its evolution in time of both the slopes and the San Lorenzo tunnel.

In the second part of this case study a description of the several steps and tools used in the attempt to add more details and information about the road tunnel damages and their status is reported. Starting from the previous works and

research (Ampezzan, D., 2017; Tedesco, G., 2018; Marcato, G. et al., 2021; Marcato, G., 2007), firstly an adequate and wider visualization of the actual state of the most damaged portions of the road infrastructure has been reached thanks to the use of proper software. Then the attention has been addressed to the stresses and forces acting on the road tunnel's aforesaid portions under examination. Thus, following the process of acknowledgement of the overall conditions related to this case, the first steps in the developing of a FEM model of a section of the above-mentioned San Lorenzo tunnel have been taken, with the help of a conveniently selected software. This latter process involved a significant number of assumptions and considerations, that ended up in what can be deemed as a beginning for further developments, which will include, step by step, more details of the complex nature of the displayed case. Nonetheless, some preliminary results are shown in order to both demonstrate the goodness of the early assumptions made and clarify what will likely be the future of this work.

A few trials, as a matter of fact, have been performed in the attempt of reaching a response by the modeled structure relatable to a loaded cantilever behavior. This kind of performance, hypothesized by Marcato and Bossi (2017), has been searched following a trial-and-error procedure in the development of few distinct models of the road tunnel structure, differing in the construction details and, in particular, in the constraints and loading arrangement. The way the discussion of the first outcomes has been carried on elucidated once again the desirable workflow for future developments.

San Lorenzo Tunnel

General outlook

The Tagliamento valley, located in the Northeastern Italian Alps of the Friuli-Venezia Giulia region, has a well-known history of slope instability phenomena (Marcato, G., 20017). Nevertheless, its strategic position from an economical point of view forced the authorities to design mobility and transportation infrastructure crossing the area. So, since there were no other feasible solutions, on the left bank of the valley the road named SS52 “Carnica” was built (Fig. 1). This road, connecting the two municipalities of Forni di Sotto (East) and Ampezzo (West), in the province of Udine, was tortuous and soon affected by intermittent rock falls and snow avalanches. Despite the implementation of road safety devices, in 1992 a double-lane road tunnel was designed as a variation of the previous route.

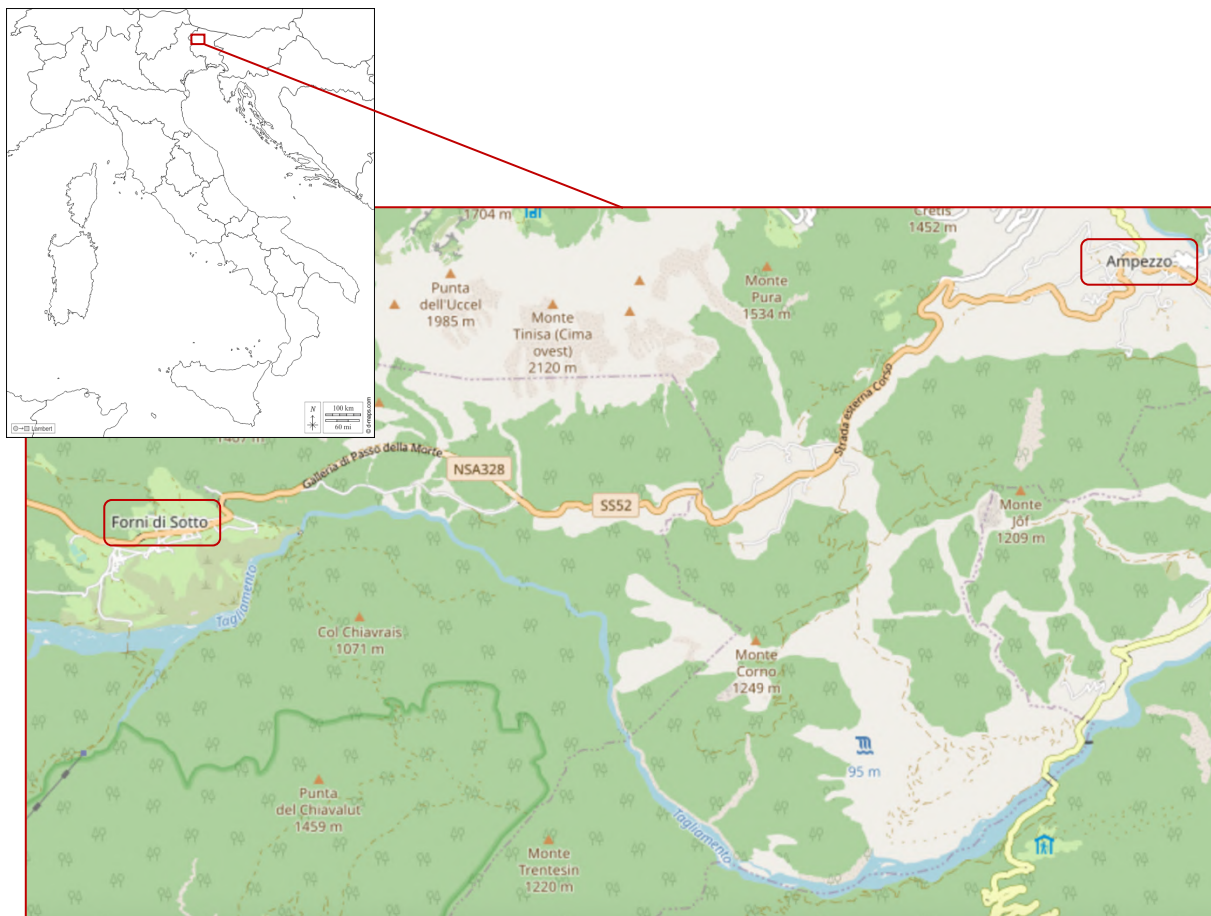


Figure 1 – Geographical map of the interested area (Openstreet Map)

The tunnel, named San Lorenzo, about 2200 m long, started to be constructed in 1994 following the New Australian Tunneling Method (NATM). Shortly after the completion of the works seepage and significant damages occurred, compromising serviceability and safety, and the road was closed. These kinds of issues were mainly reconducted to the effect of a major landslide, whose fault plane crosses the tunnel at 300 m from the entrance on the Ampezzo side. Thus, between 2005 and 2008 the first portion of the road, about 400 m, was reconstructed using a succession of 12 m long independent segments, provided with radial drains from the outermost part of the upper cap. The principle behind the use of independent segments came from the slow nature of the landslide's movements, and allowed an effective dissipation of the consequent deformations. For what concerns the encountered seepage issues, in addition to the radial drains installed around the road tunnel, a drainage adit was also realized. This T-shaped conduit, located 30 m under the road, coupled with the action of the drains, had the purpose of collecting the water flowing close to the outer part of the road tunnel in order to both limit the seepage phenomena inside the road and reduce the landslide displacements.

In the last years of activity, the abovementioned solution of the independent segments, adopted for the road reconstruction, has been effective in dissipating landslide induced stresses. On the other hand, the drainage adit turned out to be oversized with respect to the amount of water collected. This led to a moderate overall reduction of landslide displacements and to the development of some damages, like the spall and fall of pieces of concrete, posing a significant hazard for traffic. Therefore, the involved authorities had to take care of this renewed dangerous situation and to further investigate the overall scenario in which the tunnel is inserted. In particular, identification, detection and quantification of damages became necessary, and to do so a Structural Health Monitoring (SHM) network was designed and put in place. The positioned instrumentation coupled with the carried-out procedures generated a huge amount of data that helped the authorities to extend the overall knowledge about the ongoing status of both the slopes instability and the San Lorenzo tunnel infrastructure, and, where it was possible and reasonable, to design safety-increasing solution.

In the joint attempt to gain pieces of information about this situation, the present case study is part of a number of academic works and research, developed starting from the outbreak of the first issues in the construction phase. It specifically points at a deeper understanding of the landslide generated forces and stresses behind the cracks' evolution, through a backward analysis that starts from the current damages' status on the vault of the road tunnel.

Geographic site

The Tagliamento valley takes its name from the homonymous river, which is the main watercourse of the area, flowing few meters South with respect to the abovementioned road. The area where the valley is inserted is part of the Carnic Alps, renowned for slope instability phenomena, recorded since many centuries ago. As a matter of fact, in the study site five distinct landslides were mapped (*Fig. 2*). The biggest one is commonly known as Passo della Morte landslide, also called Landslide 3, and is the one mainly responsible for the issues experienced in the San Lorenzo tunnel. The name of this landslide comes from the narrow gorge nearby the detachment area, which took it in turn from an unfortunate historical event. Indeed, during Italian Risorgimento Austro-Hungarian soldiers ambushed some Italian ones, who ended up badly, hence its name, literally Death Pass.

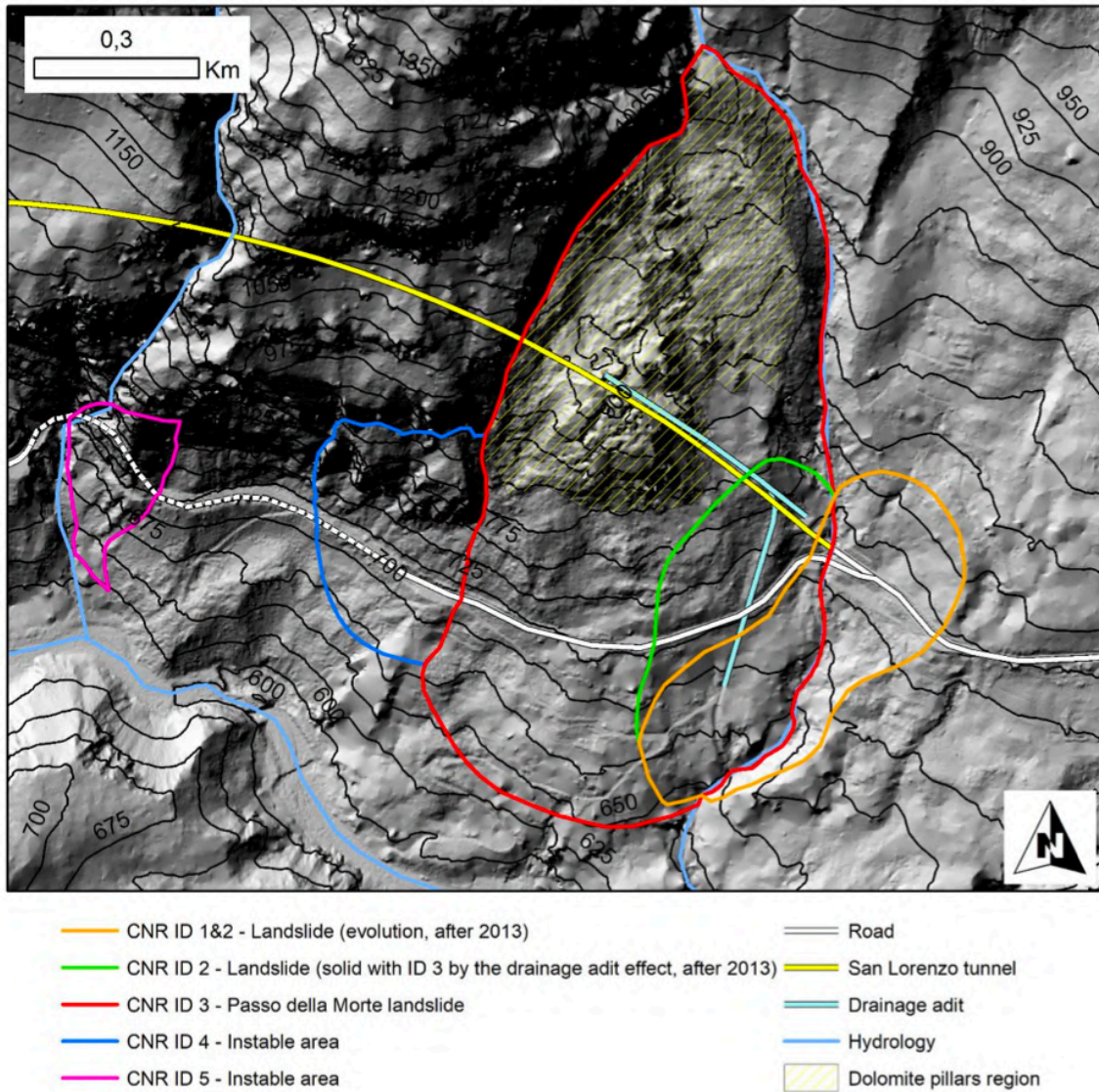


Figure 2 – Landslides in the San Lorenzo tunnel surroundings (Tedesco, G., 2018)

Friuli-Venezia Giulia region is mainly characterized by mountains and geomorphological peculiarities, like karst phenomena, which severely influenced human infrastructures and needs ever since. Nevertheless, it plays a fundamental role from an economic point of view, both on a national and international scale, as it represents the principal connection mean between Italy and Balkan countries. Therefore, despite the numerous and inherent difficulties, mobility of people and goods has always been a priority for the governance and the authorities. Thus, in the presented site of interest of this case study, the necessity of designing and building a new road tunnel was clear, since there are no other possible routes to cross the valley, except the old and dysfunctional one.

Geologic and geomorphologic setting

As mentioned before, the study area is part of the Carnic Alps. This mountain chain is south verging, characterized by a N-S compressional thrust due to the Alpine orogenesis. In the area, several Quaternary deposits, formed during pre-, sin- and post-glacial events, outcrop over a Triassic basement. They are the result of a complex erosive action triggered by glacial and gravitational processes during the Pleistocene and Holocene. In the following list, a brief description of the lithological units outcropping and of their most relevant aspects is given (*Fig. 3*):

- *Schlern Dolomite (Upper Ladinian)* – composed by light grey limestones or dolomitic limestones; overall heavily fractured since it is the roof portion of the Sauris Line, exposing it to paleo-karst phenomena; it has a variable thickness of 200-300 m; it forms the slopes of Col Pimin and Clap di Lavres right above the SS 52 road
- *Stratified Dark Limestone (Carnian)* – it consists of a succession of micritic limestone, with a variable thickness between 10 cm and 1 m, and dark marl 20 cm thick; the overall thickness of the unit is about 100 m and it covers the Schlern dolomitic one, as it can be seen from the SS 52 old route; due to presence of marl layers, slips between the different rock formation of this unit and with respect to the Schlern unit have occurred, contributing to increase the risk of slope instability in the old route
- *Stratified Limestone and Dolomite (Carnian)* – comes as a succession of limestone, dolomite and calcarenite, with some grey marl infiltrations; characterized by a thickness of 20-25 m, it outcrops along Tagliamento river
- *Massive Crystalline Dolomite (Carnian)* – formed by light grey doloarenite 10 m thick, placed right above the previous unit, encountered in the same location
- *Multi-colored Silty Clay (Carnian)* – this unit is mostly composed by reddish silty clay and siltstone with sporadic infiltrations of sandstone and marly dolomite 1 m thick; the unit overall thickness is 100-150 m, and its outcrops are small and spread; it appears very fractured since it is situated under the Sauris line

- *Gypsum (Upper Carnian)* – it is characterized by the presence of clayey impurities spread uniformly
- *Holey Dolomite (Upper Carnian)* – consists of a succession of grey marly dolomite, light tone dolomite and dolomitic marl
- *Forni's Dolomite (Norinian)* – it appears with a clear stratification of dolomite, dark marly dolomite and marl rich of organic material
- *Quaternary Deposits* – include glacial moraine, alluvial deposits, polygenic conglomerates and chaotic deposits with various degree of sedimentation, like the ones derived from the Marocca di Sacrovint, a late-glacial landslide, that caused the damming of the valley and of the Tagliamento river

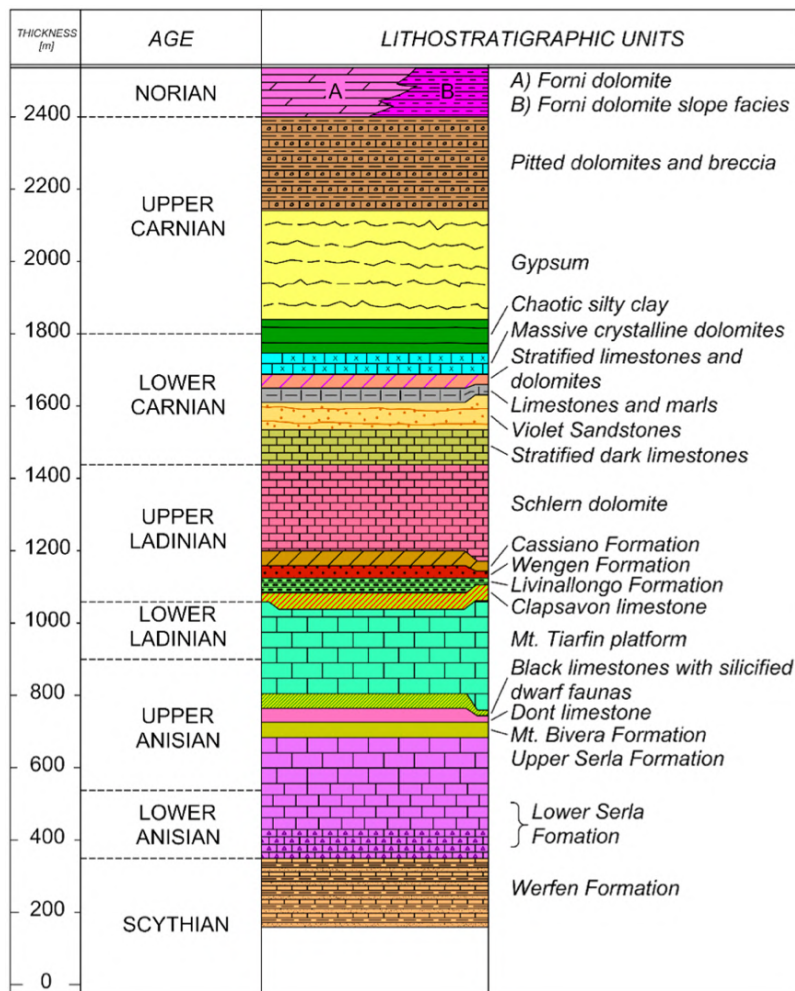


Figure 3 – Stratigraphic succession (Tedesco, G., 2018)

The presence of E-W oriented faults characterizes the analyzed area. These structures all together as a group are called Sauris Line, which is a tectonic

dislocation generated by Neogenic deformations and influenced by Triassic extension phase. It has been detected in the upper Tagliamento valley as a low angle overthrust from which the Carnian and Ladinian units, like Schlern dolomite and dark stratified limestone, overlap the ones belonging to the Upper Carnian, like gypsum and multi-colored silty clay.

Climate

The study area is characterized by a mild climate, strictly related to the sun exposition. Since the valley is E-W oriented, cold winds are the most dominant ones, generating cold winters, also with temperatures below 0 °C, and shorter cool summers. Rainfall concentrates during summer and autumn while reduces in spring and winter. The area is not new to significant rainstorms affecting and triggering slope instabilities, especially when percolating water reaches clay units. A worth-mentioning one is called Vaia, happened in late October 2018, which caused damages on the entire Nord-eastern portion of Italy, involving Lombardia, Trentino-Alto Adige and Friuli-Venezia Giulia regions, up to also the San Lorenzo tunnel. Snowiness is a relevant meteo-climatic agent too. Snow cover is persistent during winter season while it starts to melt in March/April. The presence of a consistent snowpack coupled with the worsening and enlargement of the cracks' pattern of the road tunnel, generated a new potential threat for structural health represented by frost-thaw cycles; a sudden temperature change can lead to snow melting, in the first place, and then, as the temperature changes again, to its solidification into ice, which worsens structural damages due to volume increment.

Hydrology

The main entity of the area from a hydrological point of view is the Tagliamento river, which crosses and shapes the valley and the slopes. It flows at an elevation of 660 m.a.s.l. with a 2% mean slope, on a streambed composed of limestone and dolomite, following a winding path due to the presence of landslides' accumulations, foremost the Marocca of Sacrovint ones. The river network is composed by tributaries of Tagliamento river, which are mostly mountain torrents perennial or ephemeral. Among these, Rio Verde and Rio

Scluses deserve to be mentioned as the most relevant with respect to the overall drainage system in the study area (*Fig. 4*). Both waterbeds of these streams are influenced by tectonic and stratigraphic geological features. The first one flows on the East side of the Passo della Morte landslide, reaching the road tunnel entrance on the Ampezzo side, and triggers two landslides of smaller entity, known as Landslide 1 and Landslide 2. Indeed, due to the high infiltration coefficient of these landslide bodies, the groundwater level increases, and the water table reaches the slip surface, setting off deformations and displacements. The second stream is located almost 200 m with respect to the opposite entrance of the San Lorenzo tunnel, and it is considered the main recharging mean of a spring located in the central portion of the tunnel.



Figure 4 – Stream network (Openstreet Map)

As a result of the lithological setting, the valley is characterized by a main flow direction extending from Mount Tinisa (North) to Tagliamento river (South). In fact, the Sauris line represents the contact between limestone and dolomite

units and the underlying clay-rich unit. The limestone and dolomite units are fractured in a network of joints and faults, allowing water to flow through, making them act like an aquifer. Coupled with the aquiclude action of the silty clay unit below, groundwater percolating into carbonatic rock mass and reaching the slip surface, represented by the contact line, can be considered as one of the most relevant provoking factors for the landslide phenomena in this part of the area and, so, of the damages on the road infrastructure. This mechanism of water infiltration is witnessed by the abovementioned spring, located at 800 m from the East portal, which is recharged also by Rio Scluses's infiltrated superficial water. The capital importance of determine the water table in the dolomitic rock mass shoved the authorities in charge to restore a piezometer named I20, previously dismissed. This item allows to estimate the delay between rainfall events and water table rising.

Passo della Morte landslide

In the study area five different landslides were identified (*Fig. 2*), three of which have already been mentioned. The largest one and most relevant for this case study, the Landslide 3, has been classified as a rock block slide of about 27 million m³ of material over an extension of 450 thousand m². It stretches from 1000 m.a.s.l at the scarp to 600 m.a.s.l at the toe. It has a drop shape, bordered by Rio Verde stream on the East flank and by Col Pimin on the upper West side, with the detachment scarp still clearly visible nearby the upper portion (*Fig. 5*). Thanks to the monitoring activities carried out through the years, it has been possible to understand the actual positioning of the slip surface, located at a depth varying between 200 m in the central portion and 20 m at the foot.

A reconstruction of the evolution of this landslide dynamics has led to claim that it started from a sackung following vertical faults with East-West direction, generated by the regional overthrust between the dolomitic and clay units. Then, nowadays, an ongoing overall South–South-West movement may be inferred and presented as a lowering due to the load of the mass itself, compounded by the presence of infiltrated water, and to the own properties of the two units in contact. As a matter of fact, the clay unit has been deformed too and it is following the aforesaid direction towards the Tagliamento river.

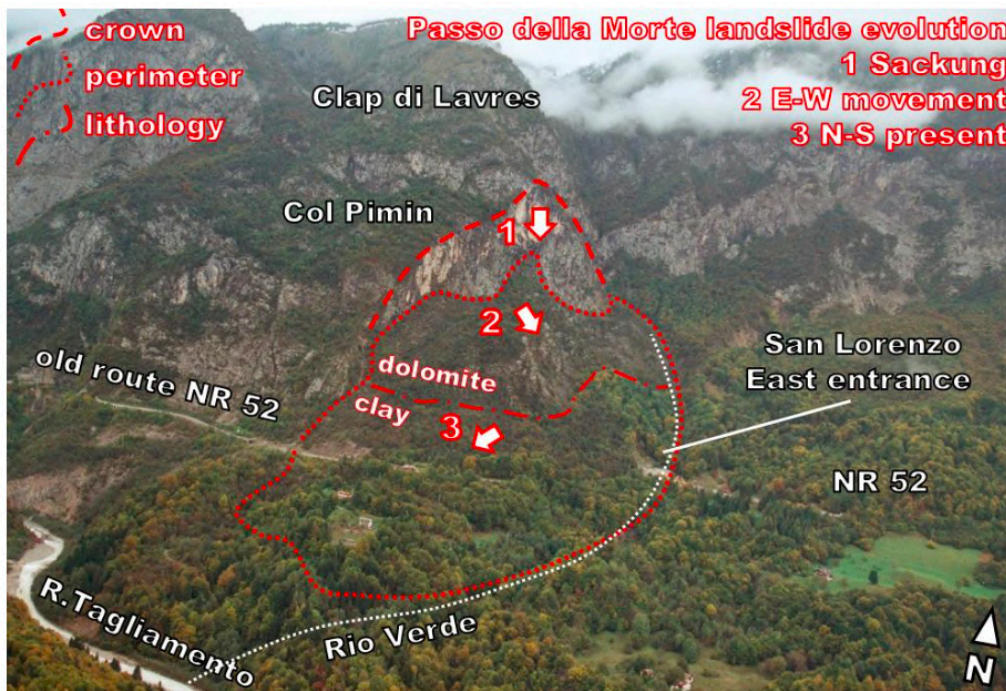


Figure 5 – Passo della Morte landslide evolution (Tedesco, G., 2018)

Just like it was previously explained in the hydrological dissertation, the presence of groundwater flowing above the slip surface can be considered the major cause of the slope movements. The previously mentioned mechanism related to the network of faults in the carbonatic unit triggered during heavy rainfall events, coupled with an almost constant water flow witnessed by springs in the area, justifies the degradation of the underlying clay-gypsum bedrock. The excavation of the road tunnel probably added even more instability to this overall framework.

State of art

Since the construction works in 1994-1996 water seepage and concrete flakes detachments occurred. For these reasons, works have been stopped from 1997 to 2006, for further investigations and monitoring. In this way springs, like the one at 800 m from the Eastern portal, were found and a global picture of the water network previously described was given. Consequently, a drainage conduit with an in plan T-shape was designed and built under the road, and a system of radial drains of almost 30 m each were drilled around the upper external cap of the tunnel to collect percolating water and prevent seepage. The drainage adit is

located about 30 m below the road tunnel, running almost parallel to it for 250 m towards West and 50 m towards East with respect to the connection point between these two branches. The remaining branch develops for 246 m almost perpendicularly to the above tunnel, with its entrance located towards the Tagliamento river at an elevation of 690 m.a.s.l. Just like the road tunnel, the adit it is also affected by several damages in correspondence of the landslide slip surface, and for this reason a proper monitoring system was installed. To increase the water drainage, several 30 m long drainpipes were installed to the adit too. Unfortunately, most of them are dry or malfunctioning because they intercept gypsum layers, which cause their obstruction by deposition of minerals. On the whole, it appears clear that the conduit is oversized, since the observed flowrate is about 18.8 l/s, way too low with respect to the one for which the conduit was designed. This happens because the adit crosses the clay-rich unit and ends up in the transition zone between clay and fractured dolomite units, failing to reach the larger water amount contained in the fractured dolomite. On the other hand, it has still helped in slowing down the landslide L2, as it is demonstrated by the data from the monitoring.

A possible improvement, that is now under consideration, is the extension of the branch under the road tunnel running towards West of about 200-250 m, thus reaching the fractured dolomite positioned right after the clay-dolomite transition zone (*Fig. 6*).

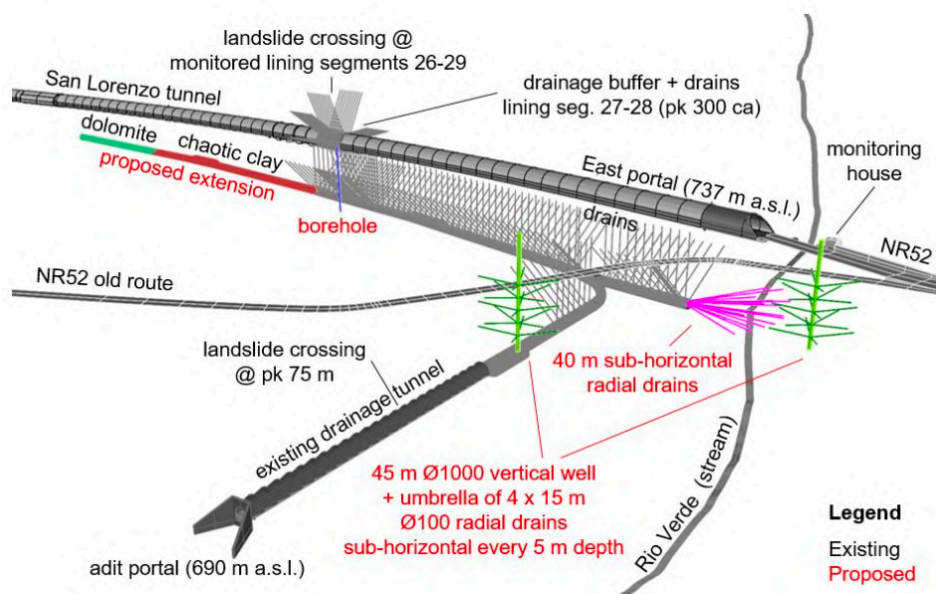


Figure 6 – Global overview of the described infrastructures (Tedesco, G., 2018)

Landslide 3 is the largest slope instability phenomenon of the area and is the one damaging the most the road infrastructure and the drainage adit below. It has been evaluated that the fault plane intersects the road tunnel at 300-400 m from the East entrance, where the tunnel crosses the Sauris overthrust, in correspondence to the area between the 27th and 28th segments (*Fig. 7*). Deepening the research of the most stressed portions of the tunnel structure, segments from 26th to 29th appear to be the ones suffering the most the consequences of the landslide actions.

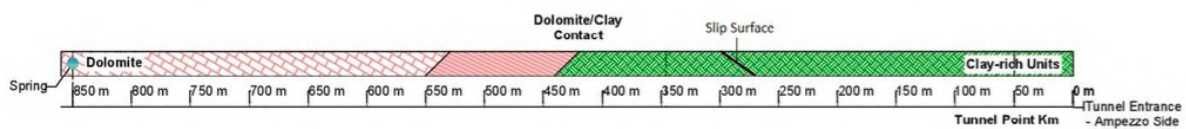


Figure 7 – Schematization of the lithological units crossed by the road tunnel (Ampezzan, D., 2017)

Fractured dolomite is a threat for the structural health of the tunnel: water infiltrates into the faults, reaches the tunnel outer part and damages it. In addition, wet dolomite rock mass exerts a greater force than a dry one on the road tunnel structure. Eventually, percolating water accumulates in the contact area softening the clay unit and thus triggering landslide movements.

The most stressed segments have shown to respond to stress forces presenting an extended crack pattern determined by the slow movements of the landslide. Since these movements are prompted by climatological events, water increases its role as major threat. Through the interpretation of the types of damages and displacements detected, it has been suggested that the 28th segment acts as it is constrained to the 29th segment and loose to the landslide induced movements on the other hand. This, indeed, induces a bending moment that opens the cracks. This cantilever-like behavior is furthermore confirmed by segments from the 27th in descending order, which seems to follow the leading movement set by the 28th, bending and dipping towards South.

Monitoring system

Concurrently with the beginning of the works for the SS52 variation, numerous investigations have been performed. Nevertheless, after the issues encountered during the early construction phase, all the authorities involved, ANAS (the national roads' authority), IRPI (Istituto di Ricerca per la Protezione Idrogeologica) and Regional Civil Protection (Protezione Civile – FVG) decided to improve the monitoring system and deepen the analysis.

The adopted solution of the independent segments has worked effectively for almost 10 years, but over the years some pieces of the concrete lining spalled, risking to fall and posing a relevant hazard for road users' safety. For this reason, starting from 2014, beside the existing monitoring system for the landslide body, a monitoring system has been installed also inside the tunnel, to control the evolution of the cracks on the vault of the most stressed segments. This system is composed by 24 crackmeters, 4 bi-axial clinometers and 70 m of optical fiber (Fig. 8). The crackmeter used type is a standard resistive bar displacement transducer made of stainless steel, operating from -20°C to $+80^{\circ}\text{C}$. Whereas the clinometer one is made of aluminum and has a resolution of $0,001^{\circ}$, operating from -20°C to $+60^{\circ}\text{C}$. The measurement data of these instruments are collected in real time thanks to the optical fibers displaced along the tunnel until the closer entrance and transmitted on a web-based platform, to make them more accessible and rapidly usable.

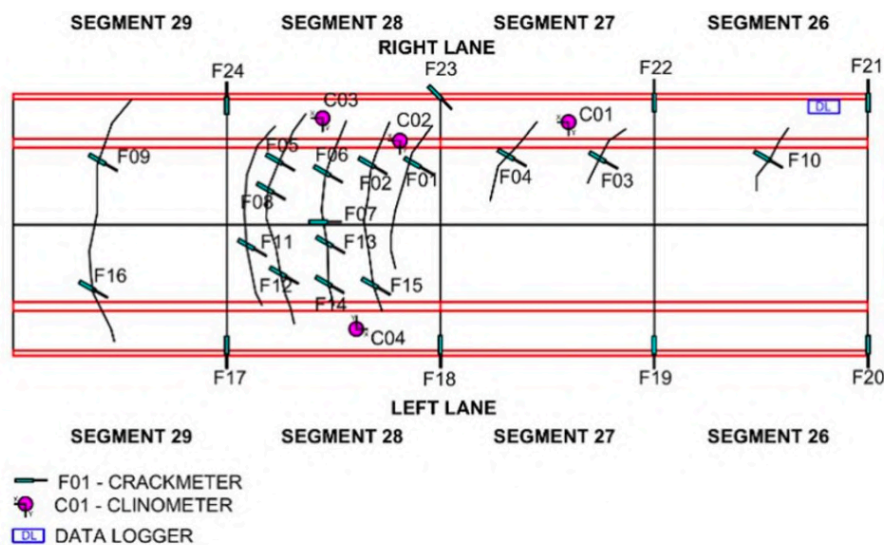


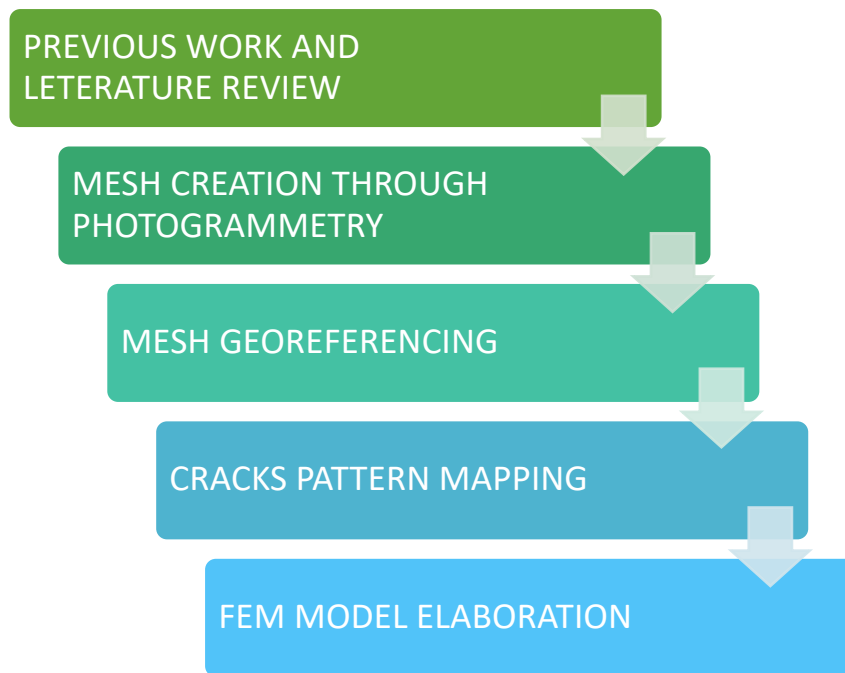
Figure 8 – Layout of the monitoring system on the most stressed segments of the tunnel

(Tedesco, G., 2018)

Analysis and Modeling: methods

As it was said at the beginning, this dissertation aims to use the continuous streak of data recorded throughout these years to put in place a reverse process that starts from the actual state of cracks, damages and displacements and tries to obtain the stresses combination which generated them. In doing so, the work has been developed through the following steps:

- *several previous works have been examined to gain a proper knowledge on the topic and on the actual progresses and activities carried out*
- *using Agisoft Metashape Pro, a software for photogrammetry, a number of photos of the vault of both sides of segments from the 27th to the 29th were converted into a mesh with a proper definition*
- *the outcoming mesh was then georeferenced thanks to a simple model created using AutoCAD, which consists of a georeferenced representation of a limited number of points of known coordinates*
- *the mesh previously created has been then opened with the software Rhino, where the graphically detectable cracks on the 28th segment have been highlighted*
- *considering the outcome of the previous phase of the work, a simplified FEM model was created with Straus7, aiming at understanding what kind of stresses, deformations, or combination of both can lead to a crack pattern like the one detected*



Mesh creation through Photogrammetry

- *using Agisoft Metashape Pro, a software for photogrammetry, a number of photos of the vault of both sides of segments from the 27th to the 29th were converted into a mesh with a proper definition*

Agisoft Metashape is a stand-alone software product that performs photogrammetric processing of digital images and generates 3D spatial data. It covers a variety of applications like GIS operations, cultural heritage documentation, visual effects production as well as indirect measurements of objects of various scales.

The software allows to process images from RGB, thermal or multispectral cameras, including multi-camera systems, into the spatial information in the form of dense point clouds, textured polygonal models (i.e. meshes) and georeferenced true orthomosaics. Typical tasks for a photogrammetry processing project in Metashape are to build a 3D surface and an orthomosaic.

In the present case study this software has been used with the purpose of converting groups of photos of the most stressed segments of the San Lorenzo tunnel into a three-dimensional mesh, such that the cracks pattern on the vault

can be graphically highlighted. Imagery data processing can be divided into these main passages:

- **Photos uploading;**
- **Alignment and Tie Points Cloud creation;**
- **Alignment adjustments;**
- **Mesh creation;**
- **Texture creation.**

Photographs suitable for 3D model reconstruction in Metashape can be taken by any digital camera as long as specific capturing guidelines are followed. Indeed, as it is well represented in the figure below (*Fig. 9*), pictures of the subject of interest should be taken aiming at redundancy. Indeed, getting more photos than required is better than not enough, since the more details the software can get the better and more reliable the outcome will be. Thus, for instance, it is recommended to avoid trying to get the whole figure of the subject in a single picture.

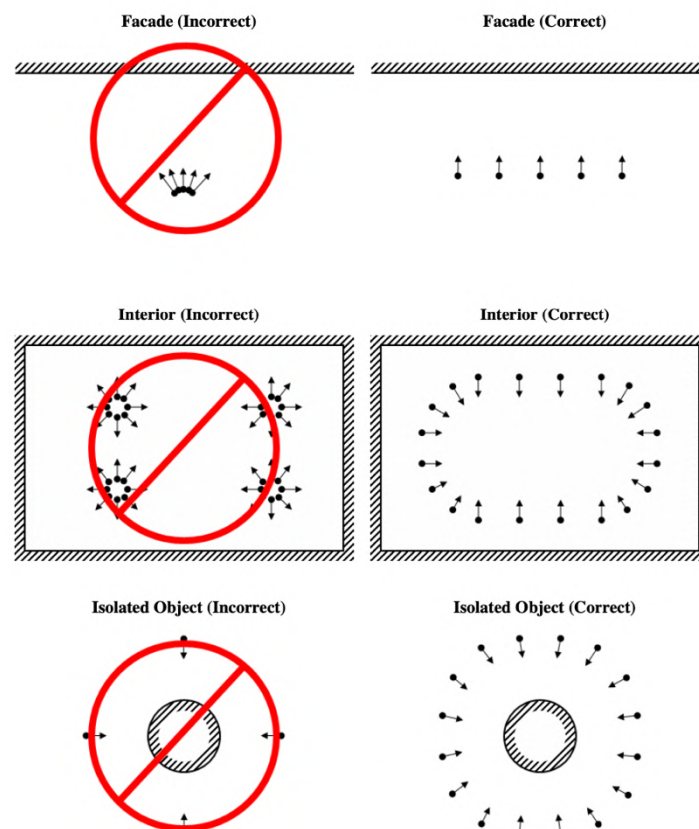


Figure 9 – General indications for cameras' arrangement (Agisoft LLC, 2022)

In the circumstances of this case study, for the whole procedure of mesh generation, the road tunnel was considered as the sum of two sides: uphill side and downhill side. This was done to avoid calculus issues and reduce the global load of the process. Two sets of photos were then uploaded for the alignment: the set of the uphill side, also called lato 2, composed by 90 photos, and the downhill side one, also called lato 1, composed by 113 photos. The images, for both sides, comprehend entirely the 27th and 28th segments and the beginning portion of the 26th and the 29th ones. Before starting any operation, it is necessary to point out which images will be used as a source for photogrammetric processing. The photos uploaded of lato 1 were all selected for further processing, while for lato 2 images were reduced from 113 to 106, discarding the less clear ones. This was done for a resolution purpose, since images characterized with bad quality can affect the overall level of detail.

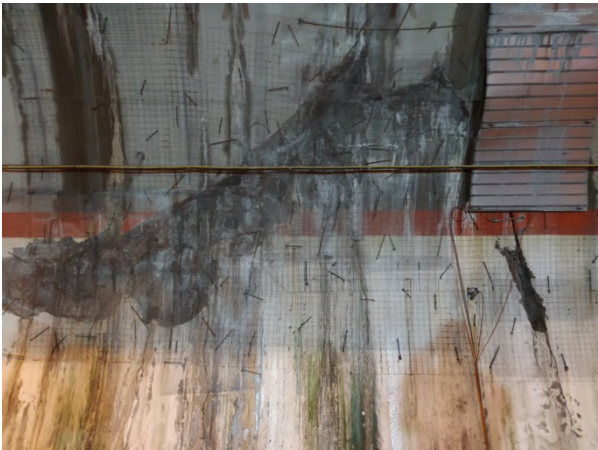


Figure 10 – Continuous streak of cameras of lato 1



Figure 11 – Continuous streak of cameras of lato 2

Through the use of aero-triangulation bundle block adjustment based on collinearity equations, exterior (translation and rotation) and interior camera orientation parameters, together with a tie point cloud containing triangulated positions of matched image points, are obtained as outcomes. The tie point cloud represents the results of image alignment and will not be directly used in further processing, but it is necessary for the determination of depth maps. Instead, the set of camera positions is required for further 3D surface reconstruction by the software.

The following parameters control the photo alignment procedure and can be modified in the Align Photos dialog box:

- **Accuracy:** options for this parameter go from Highest accuracy settings, which help to obtain more accurate camera position estimate, to Lowest settings, which get the rough camera positions in a shorter period of time; High, Medium and Low are the options in between. The main difference among them resides in the scaling factor of the original size of the photos; for instance, by selecting High accuracy setting the software works with the photos of the original size, Medium setting leads image downscaling by factor of 4 (2 times by each side), with Low accuracy source files are downscaled by factor of 16, and so on. The choice of the proper settings must be taken considering that tie points are estimated based on feature spots found on the images, so it must be related to the quality of the images themselves; it may be meaningful to upscale a source photo to accurately localize a tie point. On the other hand, higher accuracy means a more time-consuming process.
- **Key point limit:** allows to set an upper limit of points on every image to be taken into account during the processing phase. Choosing a zero value enables Metashape to find as many key points as possible, but it may result in a big number of less reliable points.
- **Tie point limit:** this number places the upper limit of matching points for every picture. Zero value means not applying any tie point filtering. This

parameter allows to optimize performance for the task and does not generally affect the quality of the further model. Nevertheless, too high or too low tie point limit value may cause some parts of the dense point cloud model to be missed. The reason is that the software creates depth maps only for pairs of photos for which the number of matching points is above a certain limit, which is generally 100 matching points.

- ***Exclude stationary tie points:*** enables Metashape to not count tie points that remain stationary across multiple different images. This option will help to eliminate false tie points related to the camera sensor or lens artefacts.
- ***Adaptive camera model fitting:*** allows automatic selection of camera parameters to be included into adjustment based on their reliability estimates. For data sets with strong camera geometry, like images of a building taken from all the sides around just as was shown in Figure 9, it helps to adjust more parameters during initial camera alignment. For data sets with weak camera geometry, instead, like a typical aerial data set, it helps to prevent divergence of some parameters.

After several attempts varying the abovementioned parameters, a combination of these has been selected and the related dialog table is shown below (*Fig. 12*).

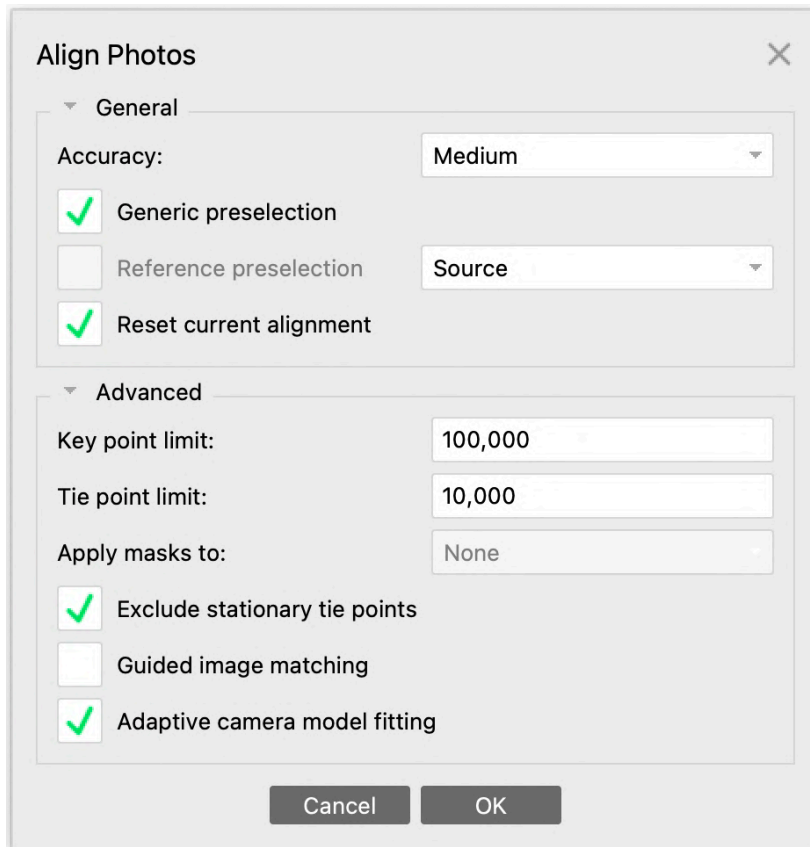


Figure 12 – Align Photos dialog box

To improve the alignment of the obtained tie points clouds, Metashape offers the chance of placing points, called markers, directly on the images. In this way, running again the alignment, it is possible to enhance the overall precision and, by giving specific coordinates to those markers, to rightly position them into space. Since the minimum number of markers to place to get a decent improvement is three, in this case study, five different markers were placed, located at key positions of the tunnel structure. The points positions used are the same for both sides of the tunnel, simply mirrored with respect to the longitudinal symmetry axis that runs parallel to the road surface, and are displayed in the figure below (Figg. 13, 14).

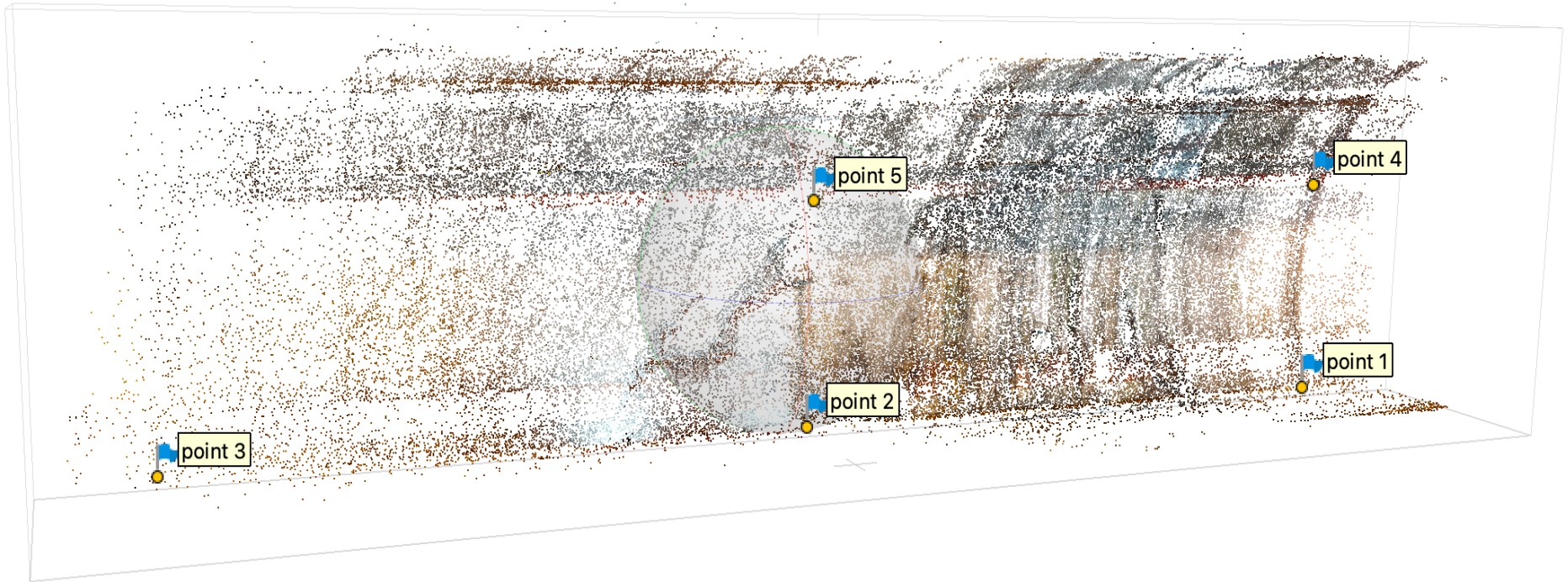


Figure 13 – Lato 1 tie point cloud with its own markers after the alignment

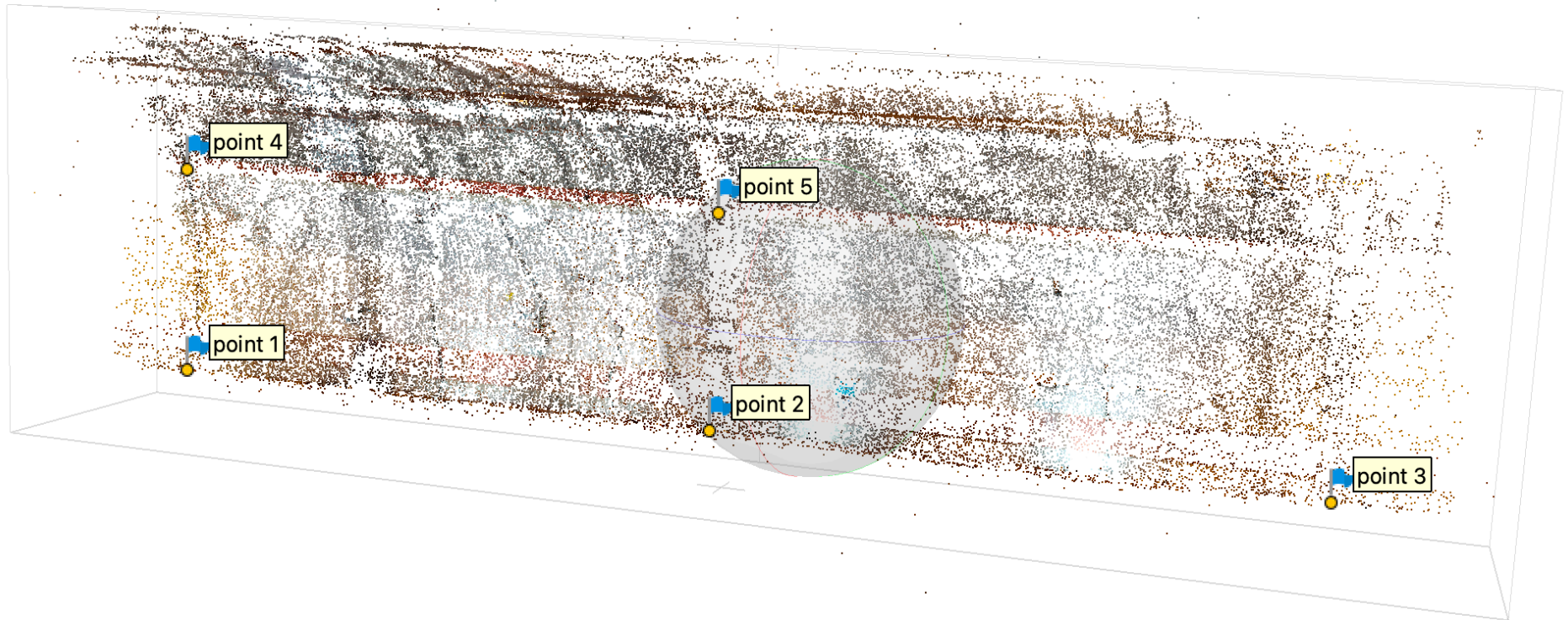


Figure 14 – Lato 2 tie point cloud with its own markers after the alignment

How the coordinates of those points were found is described in the AutoCAD sketchy model related section. After placing a marker, Metashape helps the user by automatically making a guess of where the same marker can be on all the other aligned images. Thus, the wrong guesses can be deleted, and the right ones adjusted if mispositioned. The alignment was then re-run, keeping the same parameters options shown before, to update the outcoming tie point clouds.

After double checking the position of each marker on every photo in which is present, it is good practice to resize the automatically generated region in which the tie point cloud is inserted. By doing this, noise-generated and useless points with respect to upcoming processing phases can be excluded from further processes, lowering the engaged resources.

At this stage there were two paths that could be followed:

- *Tie point cloud* → *Dense cloud* → *Mesh* → *Texture*;
- *Tie point cloud* → *Mesh* → *Texture*.

In this situation, again, a choice balancing the pros and cons of the two options has to be made. Following the first path, a more detailed result will be obtained by taking an additional step represented by the creation of a dense cloud, but it will require a much more significant amount of time to be performed. In the second path, on the contrary, time will be saved at the expense of global quality. Considering the sufficient number of images uploaded for each side and the size of the cracks with respect to the global expected frame of the output, the second path was selected.

Metashape can reconstruct polygonal mesh models based on the point cloud information or on the depth maps data. Given that the option of generating a mesh directly from the tie points cloud was selected, the software automatically generated the corresponding depth map, that, as it will be explained later, enables to reach more exhaustive results.

Mesh creation procedure is controlled by the following parameters, which can be modified in the Build Mesh dialog box:

- **Source data:** specifies the source for the mesh generation procedure. The difference in the selected source lies in the outcoming quality. Tie points, for instance, can be used for fast 3D model generation, while Dense cloud

settings will result in longer processing time but high-quality output. Depth maps settings, instead, use all the information from the input images more effectively, becoming less resource demanding compared to the Dense cloud-based reconstruction.

- **Quality:** specifies the desired reconstruction quality of the depth maps, providing that they are selected as a source option. Interpretation of the quality parameters here is similar to the one of accuracy settings, given in the alignment section. Higher quality settings, for example, can reach more detailed and accurate geometry but require longer time for the processing. The only difference is that in this case Ultra High quality settings means processing of original photos, while each following step implies preliminary image size downscaling by factor of 4 (2 times by each side).
- **Face count:** defines the maximum number of polygons in the final mesh. Suggested values (High, Medium, Low) present optimal number of polygons for a mesh of a corresponding level of detail. It should be considered that, while too small number of polygons is likely to result in too rough mesh, too huge custom number (over 10 million polygons) is likely to cause model visualization problems in external software.
- **Depth filtering:** the software calculates depth maps for every image. Due to some factors, like noisy or badly focused images, there can be some outliers among the points. To sort them out, Metashape has several built-in filtering algorithms that answer the challenges of different projects. Mild depth filtering mode is recommended if there are important small details which are spatially distinguished in the scene to be reconstructed, so that they are not sort out as outliers. If the area to be reconstructed does not contain meaningful small details, then it is reasonable to choose Aggressive depth filtering mode to sort out most of the outliers. Moderate depth filtering mode brings results that are in between the Mild and Aggressive approaches. Eventually, depth filtering can be Disabled, but it is not recommended as results could be extremely noisy. For depth maps-based

mesh generation the Mild filtering option is used by default, unless the Reuse depth maps option is enabled.

For the polygonal mesh generation, several attempts varying the abovementioned parameters were performed too; the combination of parameters eventually chosen is reported in the dialog window below (*Fig. 15*).

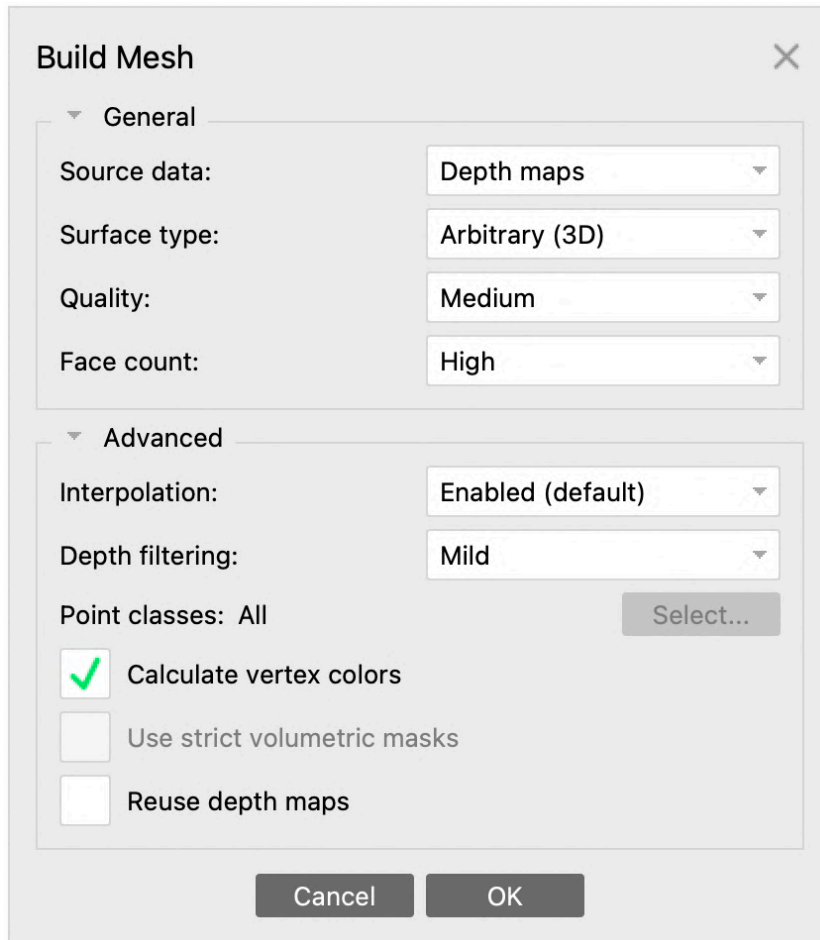


Figure 15 – Build Mesh dialog box

The final step consisted in the texture creation. Since the photos were taken with a smartphone, no adjustments were made on original color or light, even though Metashape provides a specific tool to do so, called *Calibrate colors*. For the same reason the default features setting that the software suggests has been left like it was, without changing it.

The related dialog box is reported here below (*Fig. 16*).

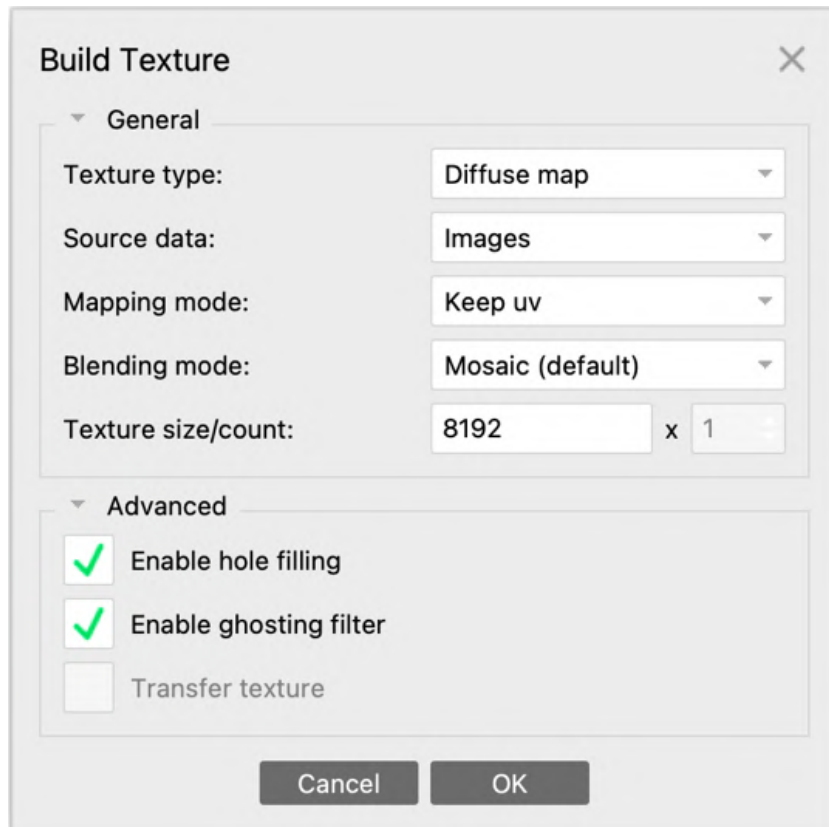


Figure 16 – Build Texture dialog box

The final results consist of two 3D meshes, one for each side of the San Lorenzo tunnel, then exported in .obj format (*Fig. 17, 18*).

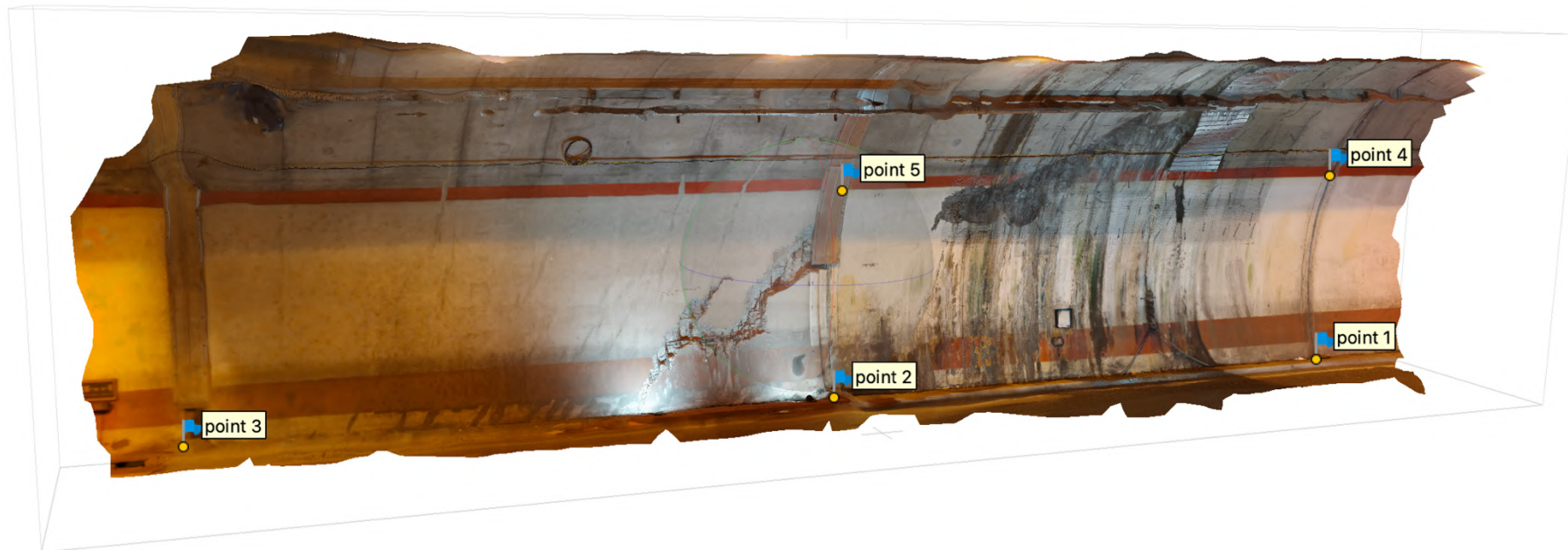


Figure 17 – Final 3D textured mesh of lato 1

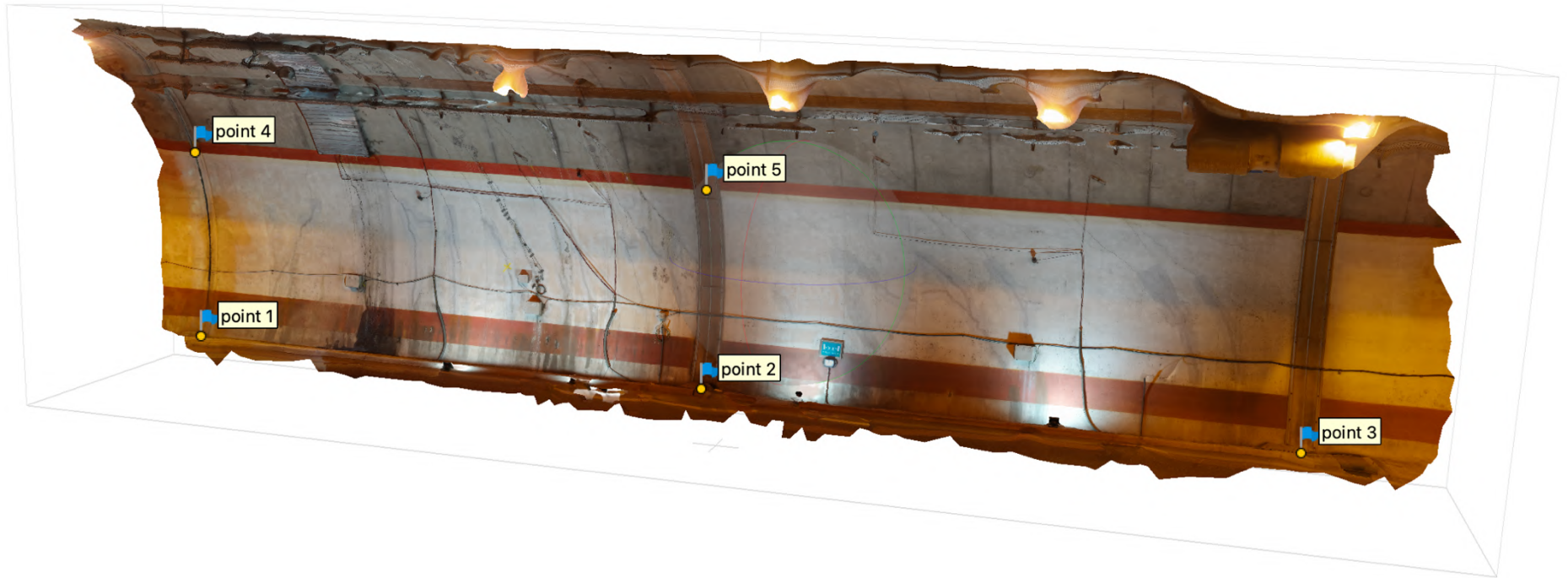


Figure 18 – Final 3D textured mesh of lato 2

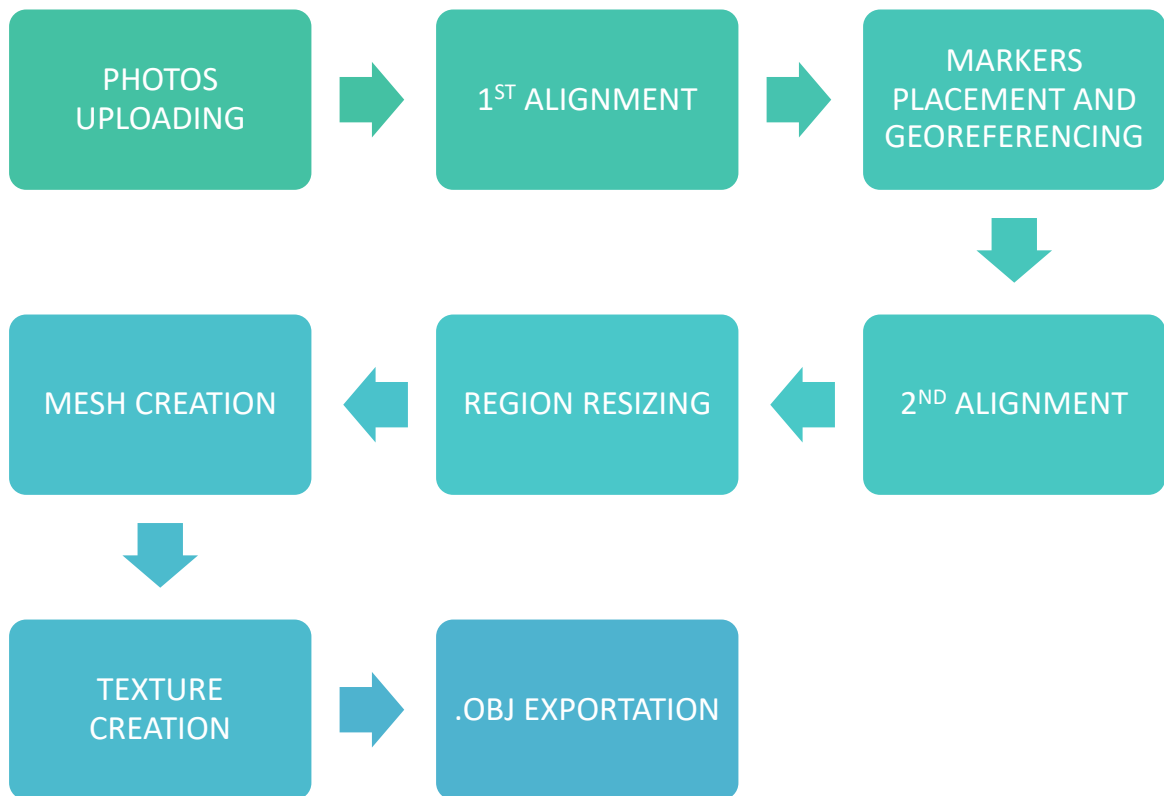


Figure 19 – Global scheme of the meshes generation step

Mesh georeferencing

- *the outcoming mesh was then georeferenced thanks to a simple model created using AutoCAD, which consists of a georeferenced representation of a limited number of points of known coordinates*

The necessity of right placing into the space the Metashape outcoming meshes of the portion of the San Lorenzo tunnel of interest was claimed by a simple model built with AutoCAD.

AutoCAD is a computer-aided design software developed by the company Autodesk, from which the program's own name is derived. The acronym CAD stands for Computer-Aided Design and defines software which enable the users to create designs of many kinds in a quick and simple way. AutoCAD, indeed, has a wide range of both 2D and 3D applications, from interior design, logos creation and fine art to engineering, architectural and aeronautical designs. Within the present case study, the purpose of the use of this software was to obtain the coordinates of the key points of the tunnel structures selected to be used as markers in the georeferencing procedure during the mesh generation on Metashape. To do so, the procedure started from the assumption that the designed length of 12 m of each independent segment has not changed in time. Three points, corresponding to the bases of the junctions between three adjacent segments, were drawn assuming one of them placed in the axes' origin and adding just a 12-by-12 m increment of the z coordinate to the remaining two. From this first three points, other two were created by adding, exclusively to the one placed on the axes' origin and to the subsequent one, an elevation of 4.15 m. To simplify the markers individuation and adjustment procedure in Metashape, points that provide both detectability ease and chance to be measured should be selected. Exactly for this reason, the chosen distance measurement of 4.15 m, taken directly on the field with the help of a laser distance meter, is the one between adjacent segments' junction and the lowest portion of a painted red band on the vault, easily recognizable on Metashape visualization. The considered global orientation of this portion of the road tunnel was measured on field as well and is about 10° w.r.t. North. It has been applied to the points created so far,

keeping the point located on the axes' origin as fixed rotation pole. Finally, all five points have been copied and pasted at the distance of 10 m, corresponding to the designed extent of the roadway. It must be mentioned that, in the reasoning behind the construction of this model, it was assumed to disregard the height of the sidewalk and the curvature of the vault.

AutoCAD allows to get the coordinates by simply checking the points properties, and these are the ones gained from the above created points (*Table 1*):

Table 1 – Key points coordinates

KEY POINTS COORDINATES							
LATO 1				LATO 2			
	X	Y	Z		X	Y	Z
1	0	0	0	1	-1.7365	9.8481	0
2	11.8177	2.0838	0	2	10.0812	11.9319	0
3	23.6522	4.071	0	3	21.9559	13.9261	0
4	0	0	4.15	4	-1.7365	9.8481	4.15
5	11.8177	2.0838	4.15	5	10.0812	11.9319	4.15

Here below the resulting 3D sketchy model is shown (*Fig. 20, 21, 22*).

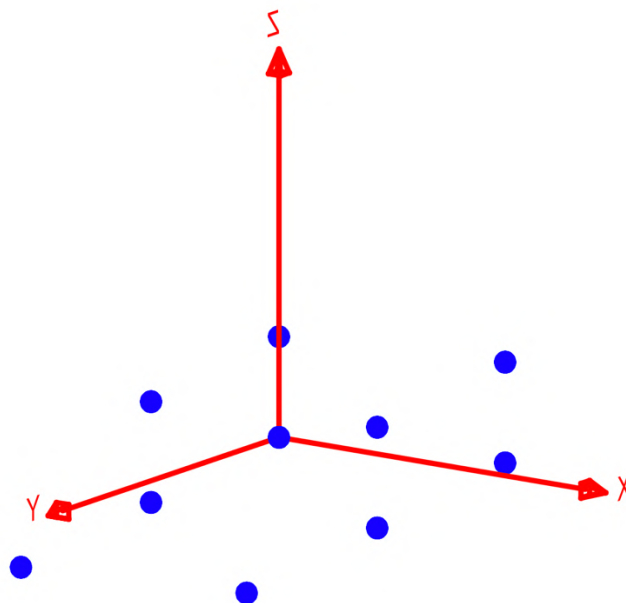


Figure 20 – Rendering of the AutoCAD model

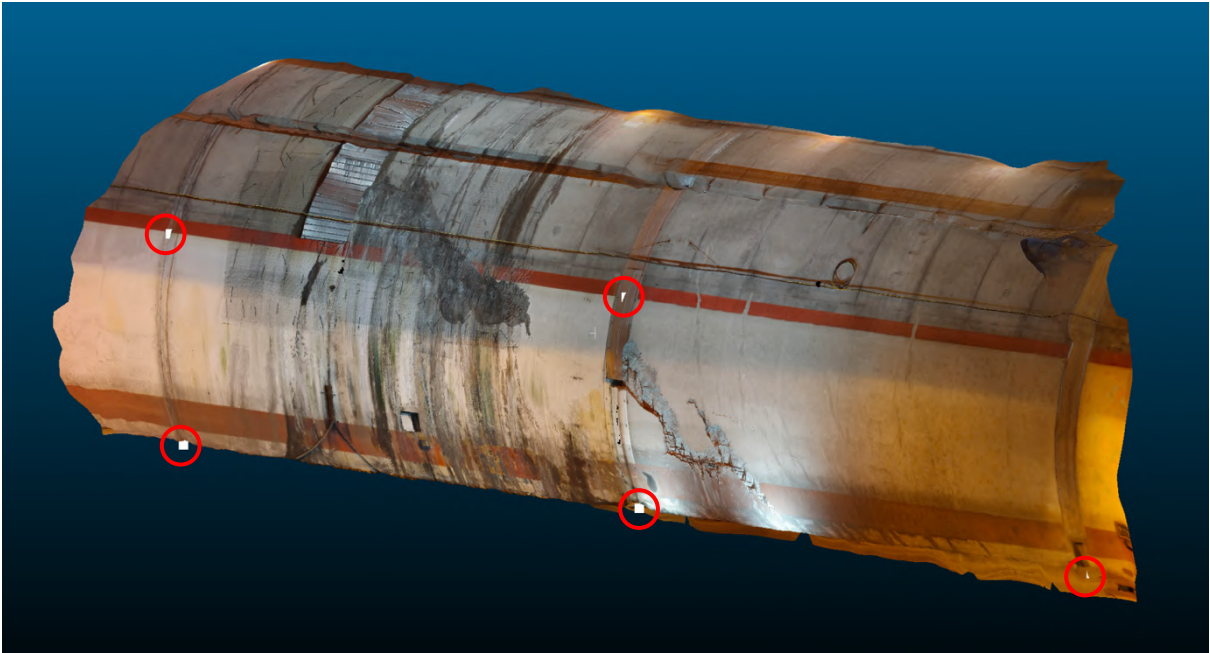


Figure 21 – Superimposition of the Metashape mesh of lato 1 and the AutoCAD model of the corresponding side, with obtained key points highlighted in red

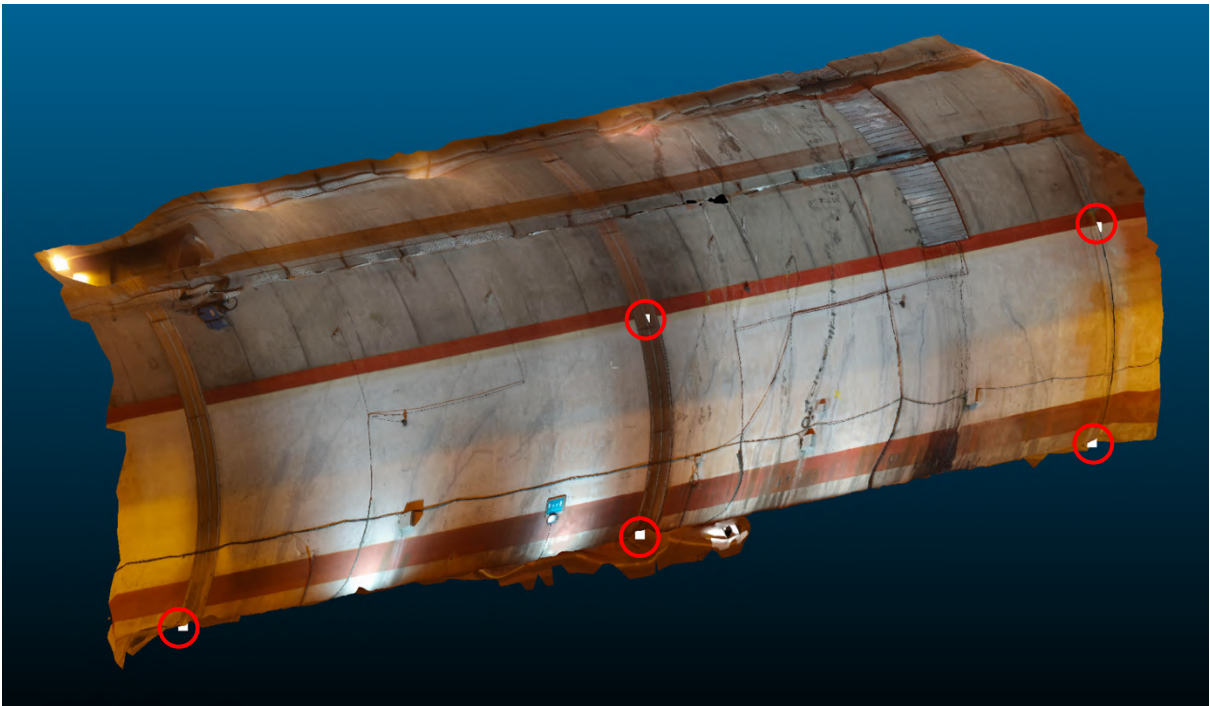


Figure 22 – Superimposition of the Metashape mesh of lato 2 and the AutoCAD model of the corresponding side, with obtained key points highlighted in red

Cracks pattern mapping

- *the mesh previously created has been then opened with the software Rhino, where the graphically detectable cracks on the 28th segment have been highlighted*

The graphic tracking of the fractures on the vault of the San Lorenzo tunnel wasn't convenient to be performed with AutoCAD, although the operation in itself could be done with this software. Indeed, AutoCAD's difficulties in managing the amount of data of the Metashape generated 3D meshes were the main source of the encountered problems. Considering that, the software named Rhinoceros3D was selected to proceed in the expected task.

Rhinoceros3D (or Rhino3D, and often simply Rhino) is one of the many 3D modelling packages on the market, very popular in the world of design and architecture, especially where non-standard geometry and data need to be processed. Thanks to this software, the user is enabled to create, analyze, edit, animate, render, document and translate surfaces, solids, polygon meshes, point clouds and NURBS (Non-Uniform Rational Basis Splines) curves. Basically, no limitations in sizes or possibilities are actually given, beside the hardware ones. This software's applications, indeed, range from industrial engineering to jewelry designing.

Originally developed to be a complement to AutoCAD, it has detached from this role thanks also to the capability of working with a larger variety of formats, becoming in some cases a conversion tool, able to overcome compatibility barriers between different software. This was a major argument behind the decision of using Rhino to continue in the processing of the foreseen goal of this phase of the case study. The difficulties experienced in managing the textured meshes were in fact easily overcome. The crack pattern was identified for both sides of the road tunnel and highlighted by the creation of a specific overlapping layer with which the fractures were traced in red. By doing so the software enables to obtain a clearer 3D visualization of the global damages' status. The ultimate results are reported below (*Figg. 23, 24*).

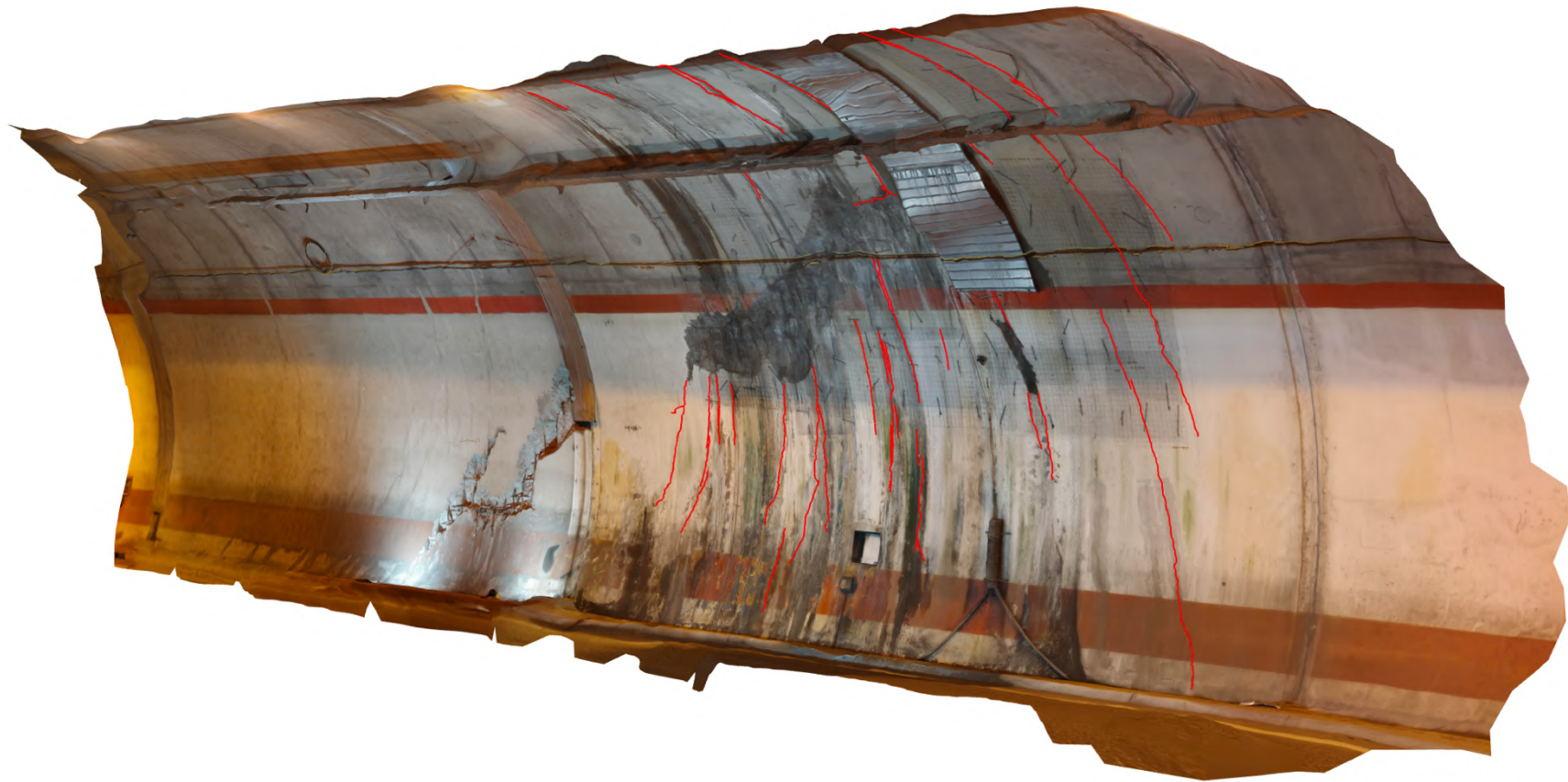


Figure 23 – Crack pattern on the downhill side (lato1)

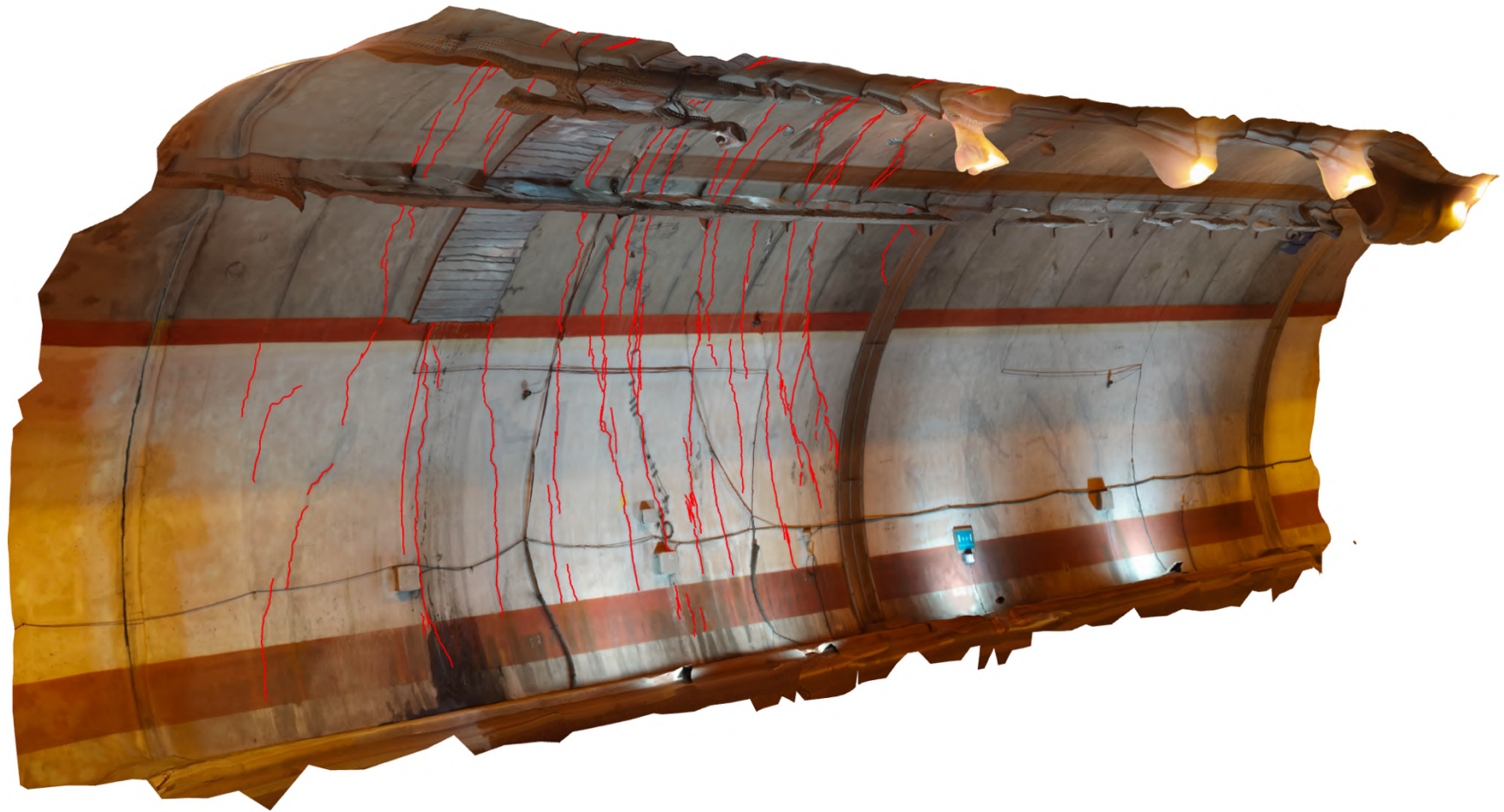


Figure 24 – Crack pattern on the uphill side (lato2)

FEM model elaboration

- *considering the outcome of the previous phase of the work, a simplified FEM model was created with Straus7, aiming at understanding what kind of stresses, deformations, or combination of both can lead to a crack pattern like the one detected*

Reaching this stage of the case study, the damages overall condition has been made clear enough to further proceed with the subsequent phase, consisting in the attempt to evaluate the stresses and forces which led to the actual condition of the road infrastructure. In order to carry out this step, a FEM (Finite Element Method) software has been used to build a coherent reproduction of the most stressed portion of the San Lorenzo road tunnel. Among the multitude of software systems based on the finite element method, the selected one is called *Straus7* (or *Strand7* outside Italy). This software provides a visual environment for applying the method to real world engineering problems. With some powerful solvers it enables the user to construct models, run analyses and investigate results simultaneously, both in 2D and 3D. Thanks to its high-standard usability it has been chosen over time by a huge number of users coming from different engineering fields, from aeronautical, automotive and mechanical to civil, biomedical and marine. A relevant feature that severely influenced the choice of this software was its capability of importing CAD-generated geometry.

A slight deepening on the general functioning behind a structural analysis performed using the finite element method is needed to better follow each step taken in the procedure applied hereafter in this case study. The process starts with the structure subdivision into a succession of domains, called elements, connected to each other by nodes, that together form a mesh. From a mathematical point of view, finite element structural analysis seeks to determine a distribution of a quantity, i.e. displacement, stress or strain, under the given loading and boundary conditions. In the procedure that leads to the obtaining of the aforesaid distribution, relationships between nodal variables, like displacement, velocity and force, are set by the mean of physics laws. To express the overall structural behavior through a number of equations in terms of

unknown variables, element matrices and vectors are grouped into global matrices and vectors. Then, those equations are solved by applying boundary conditions, obtaining in this way the values of the unknown variables, like nodal displacement, which become the basis for the further calculations to find other quantities. Thus, with this method the resulting function representing the distribution of the sought-after quantity follows the governing equations of the problem and satisfies the given boundary conditions. In addition, the function at hand is piecewise defined and is expressed in terms of its values at the nodes of the finite element model, leading to a set of linear or nonlinear equations of the nodal values of the chosen variable.

Summing up, a FEM model is a numerical model used for simulating the behavior of a real physical system, taking into account its geometric representation (*mesh*), its materials characteristics (*constitutive equations*), external loads and inner restraints (*boundary conditions*) and the solving analysis required (*solver selection*).

The presented workflow has been applied and followed in the design of the road tunnel segment FEM model. The first step taken was, though, the creation with AutoCAD of the geometry of the longitudinal cross-section of the infrastructure. In fact, producing a geometry directly in the Straus7 environment is unnecessarily intricate and easily affected by error. From the available material, in particular from the CAD table n° 4.04 – “Demolizione e rifacimento conci”, the cross-section of the entire tunnel portal has been acquired and simplified by removing the considered useless parts, in order to produce a version of it containing just its structural parts' inner and outermost edges (*Figg. 25, 26*).

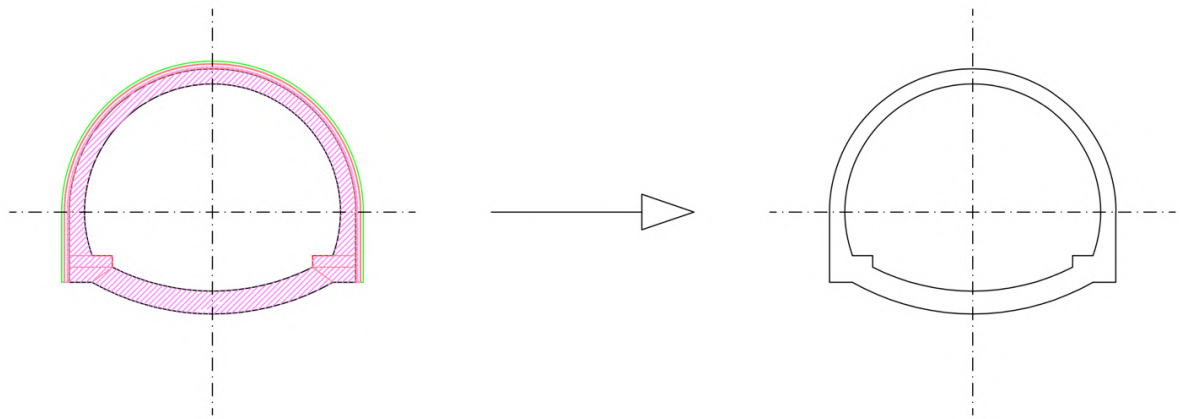


Figure 25 – San Lorenzo tunnel cross-section simplification

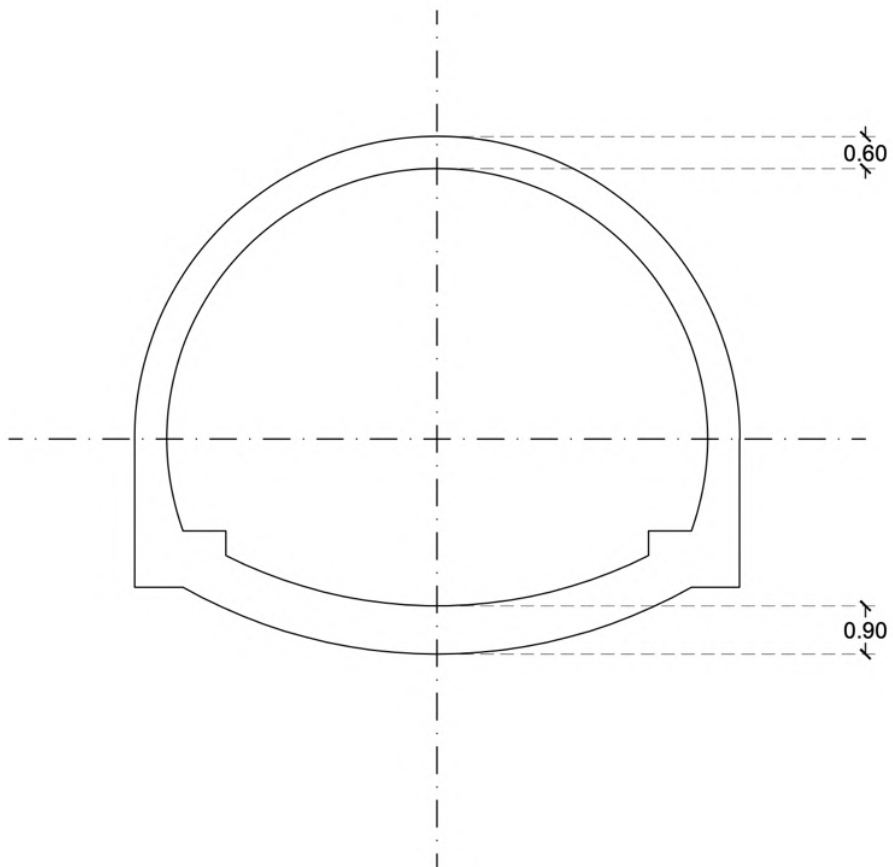


Figure 26 – San Lorenzo tunnel cross-section simplified, with semi-vaults' thickness values

The above-created cross-section geometry has been then divided into sectors by a system of concentric rays starting from the center of gravity of the section itself as shown in the following figure (*Fig. 27*).

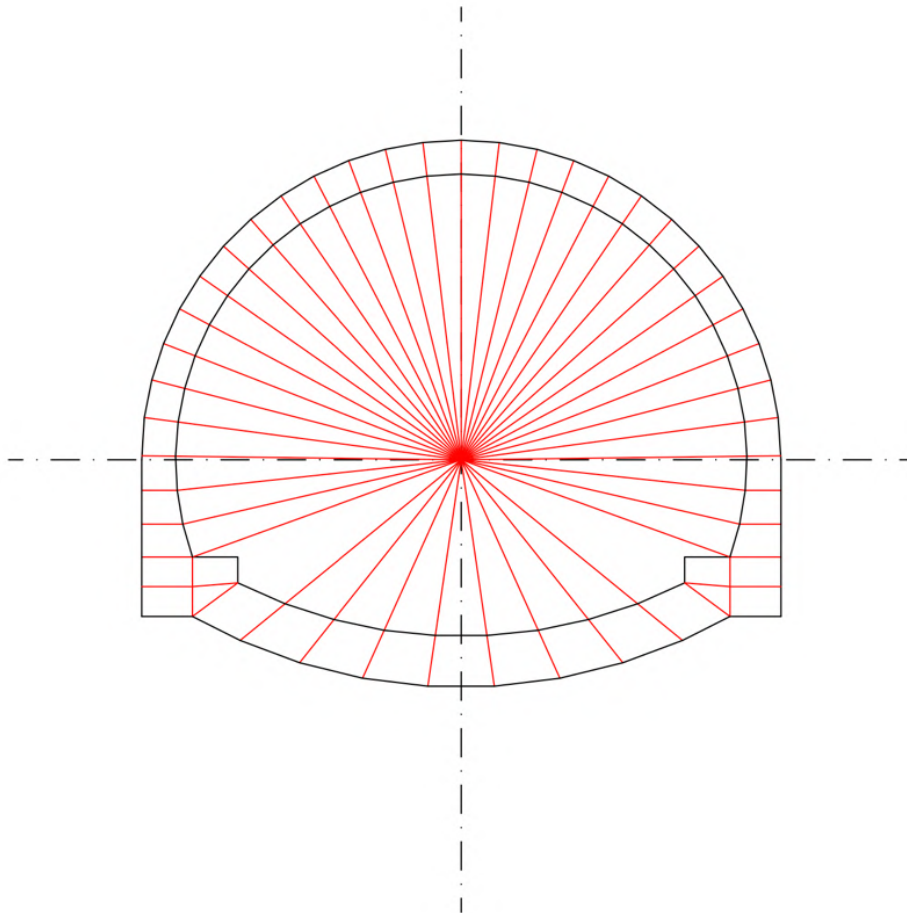


Figure 27 – San Lorenzo tunnel cross-section with divisional rays

The aforesaid rays have been drawn aiming at dividing the section into a succession of almost squared identical geometric figures. To do so, the different thickness of the upper and lower semi-vaults, reported in Figure 26, have been taken as the criterion following which the distance between a pair of subsequent rays has been set. The reason behind this procedure was trying to create plane geometric figures as similar as possible to each other, in order to reduce the possibility of error by the software in future steps, considering that Straus7 includes automatic mesh generation tools working directly from geometry.

The quest of balancing the necessity of, on one hand, create almost equal geometric figures while, on the other hand, generate a number of figures that can

cover the whole cross-section surface was extremely complicated from a practical point of view, and definitely not precisely nor entirely achievable. Thus, after splitting the arcs into a number of portions of equal dimension thanks to the CAD-provided command *DIVIDE*, the distance between rays in the upper semi-vault has been taken as near as possible to 0.6 m, while in the lower semi-vault to 0.9 m, generating in this way almost square figures in both the portions of the cross-section. As it has just been clarified, the composite and non-linear nature of the cross-section geometry made infeasible to create perfectly identical figures, especially in correspondence of the sidewalk angle on both left and right side. In those positions, accordingly, the less unpleasant solution has been adopted. The points defining the referred figures and obtained by the intersection between the drawn rays and the contours of the cross-section, will thus become nodes in the Straus7 environment.

The resulting geometry, excluding the divisional rays, has been exported as a .dxf file and imported in Straus7 (*Fig. 28*).

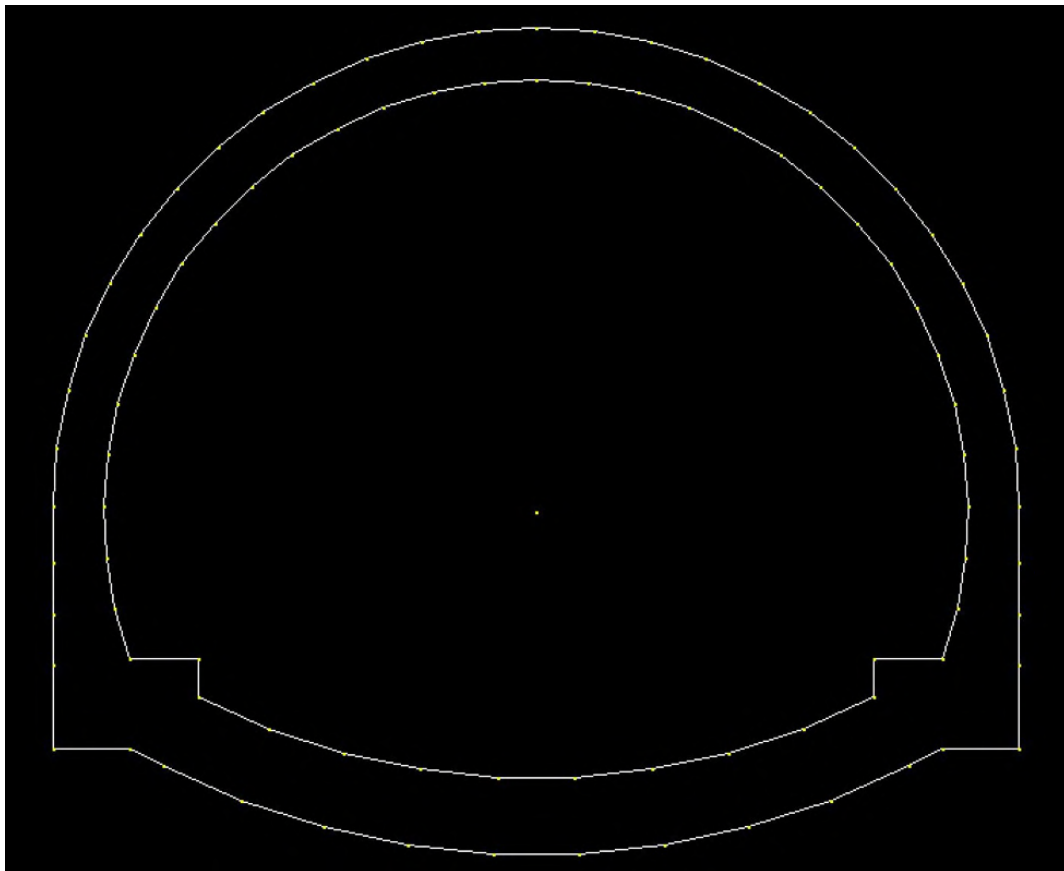


Figure 28 – San Lorenzo tunnel cross-section imported in Straus7, with the divisional-rays-procedure-resulting nodes highlighted in yellow

Here, since the software allows to automatically generate 4-node and 8-node plates from 2D regions, the points, generated with the previously described procedure carried out in AutoCAD, were linked to create a succession of plates, essentially recreating the above-mentioned plane figures (*Fig. 29*).

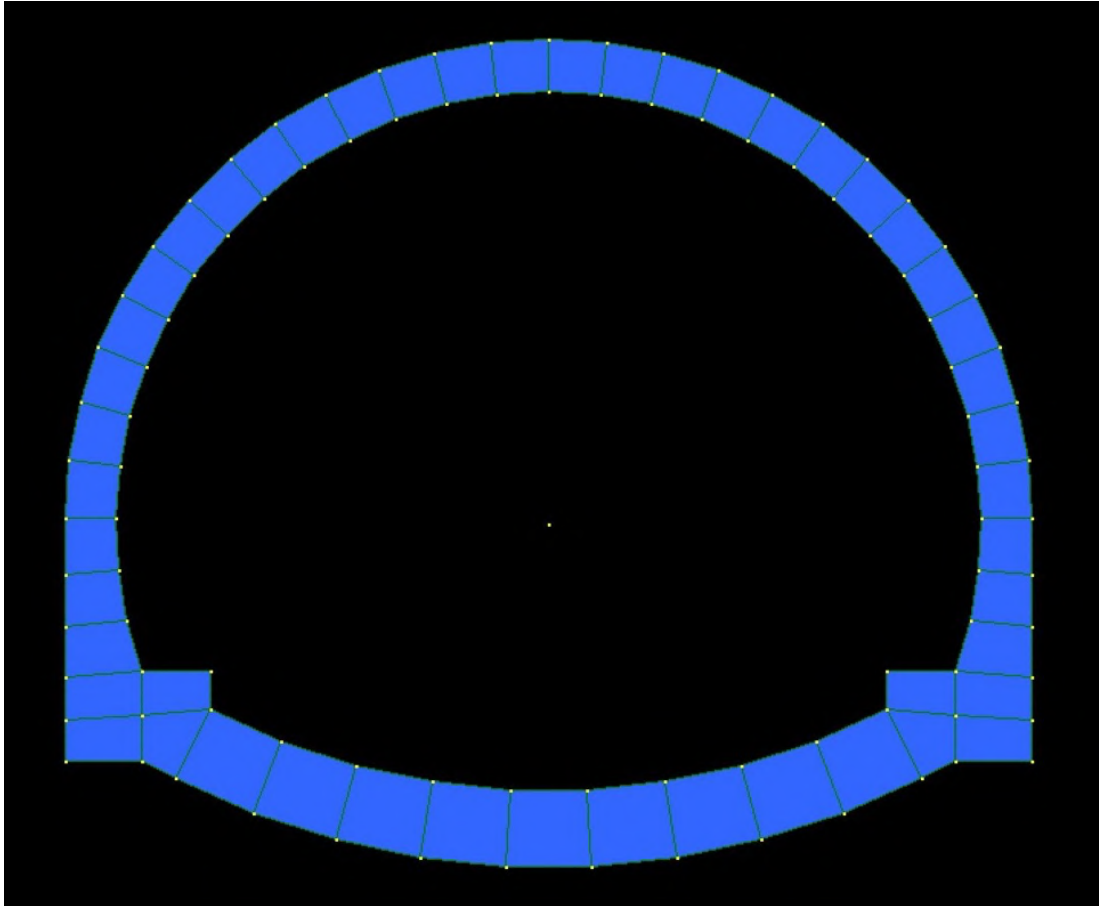


Figure 29 – San Lorenzo tunnel cross-section with Straus7-created plates

At this point, the plates were extruded, taking advantage of the dedicate option provided by the software, for a distance of 0.6 m, imposing the repetition of the extrusion process for 20 times, in order to generate, as ultimate result, the reproduction of a single segment 12 m long, composed by almost cubic elements, called bricks (*Figg. 30, 31, 32, 33*).

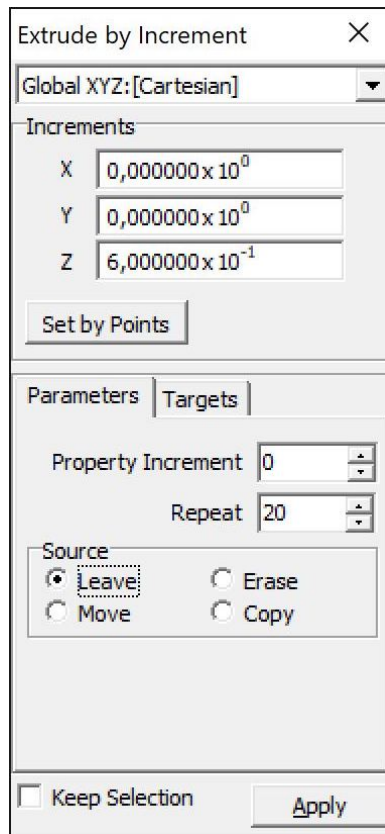


Figure 30 – Straus7 extrusion's dialog box

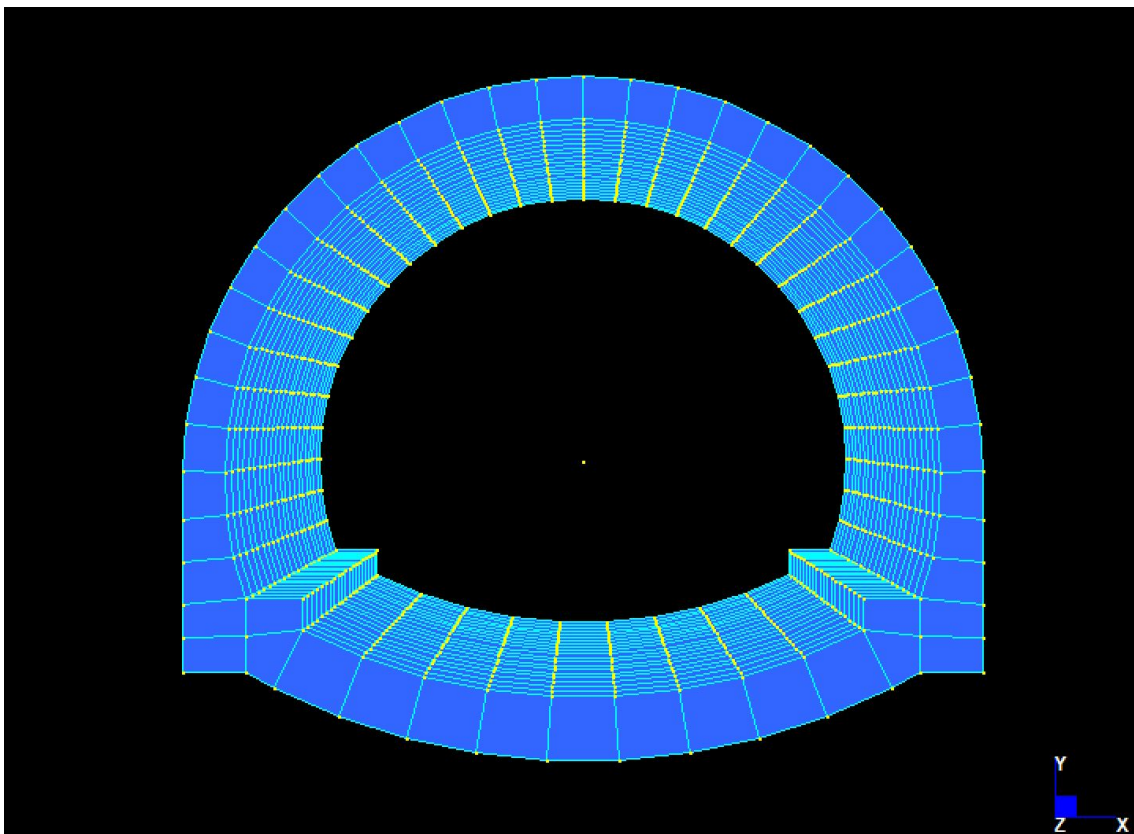


Figure 31 – 1st view of the Straus7-resulting San Lorenzo tunnel single segment mesh

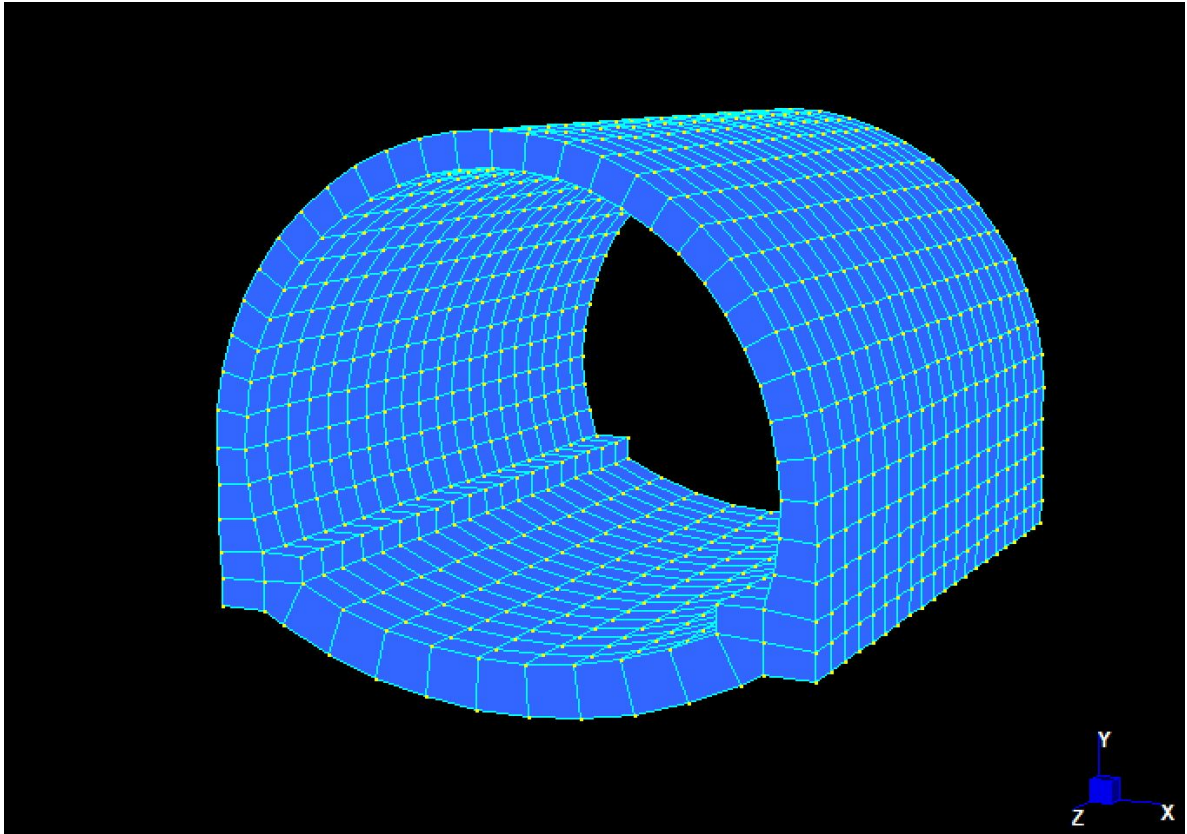


Figure 32 – 2nd view of the Straus7-resulting San Lorenzo tunnel single segment mesh

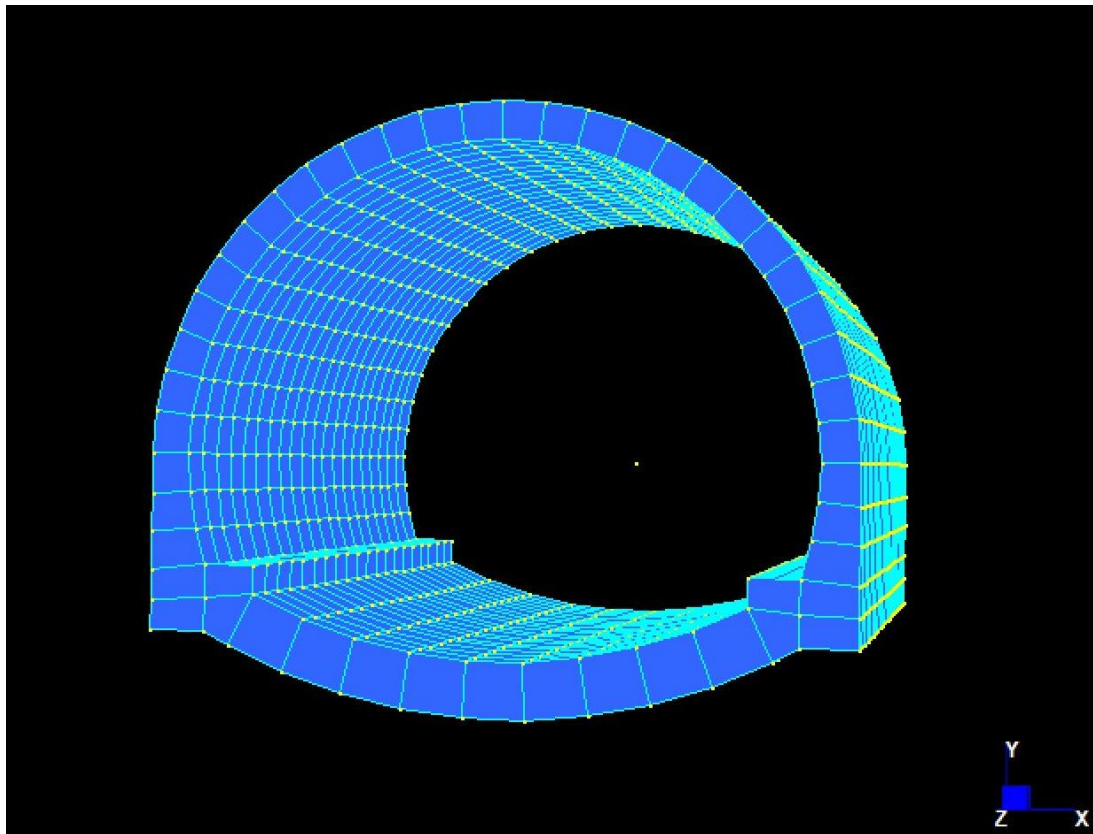


Figure 33 – 3rd view of the Straus7-resulting San Lorenzo tunnel single segment mesh

The plates previously created have been erased since they were only functional to the extrusion procedure. Considering the final achieved model satisfying, the following phase consisted in properly defining the material's characteristics and put reliable boundary conditions to the modelled segment. As in many cases in the mathematical models' development field, this delicate phase was led by uncertainty since every step taken was preceded by assumptions on unknown data or outcomes. A trial-and-error workflow was followed, with adjustments and verifications during the progression.

Since nor trustworthy nor precise information about the actually used construction material were found, otherwise appropriate characteristics were taken from the Master Degree thesis titled "*L'intelligenza artificiale per caratterizzare il degrado del calcestruzzo nelle gallerie*" (Aiello, S., 2021). In this work, through the assessment of a number of tests on different samples coming from as many road tunnels in Italy, some relevant physics parameters were derived (*Fig. 34*).

Galleria	Direzione	Massa Volumica media (kg/m³)	Tensione media (MPa)	Deviazione Standard sulla Tensione (MPa)	Velocità US media (m/s)	Deviazione Standard sulla Velocità US (m/s)	Dimens. max aggregato (mm)
Borgonovo	Ventimiglia	2251.89	16.52	5.92	3232.44	326.51	26
Cantalupo	Ventimiglia	2265.41	18.12	7.95	3629.78	329.29	28
Crevari	Ventimiglia	2153.92	12.76	4.10	3368.41	335.66	22
Monte Castelletti	Genova	2271.80	25.69	5.31	3560.01	289.00	33
Pecorile	Ventimiglia	2315.81	20.97	6.57	3710.77	311.78	38

Figure 34 – Physical/mechanical parameters of concrete samples from the abovementioned Master Degree thesis (Aiello, S., 2021)

Due to the lack of data on the effectively used material, the missing but needed ones were assumed as shown in the following dialog box (*Fig. 35*).

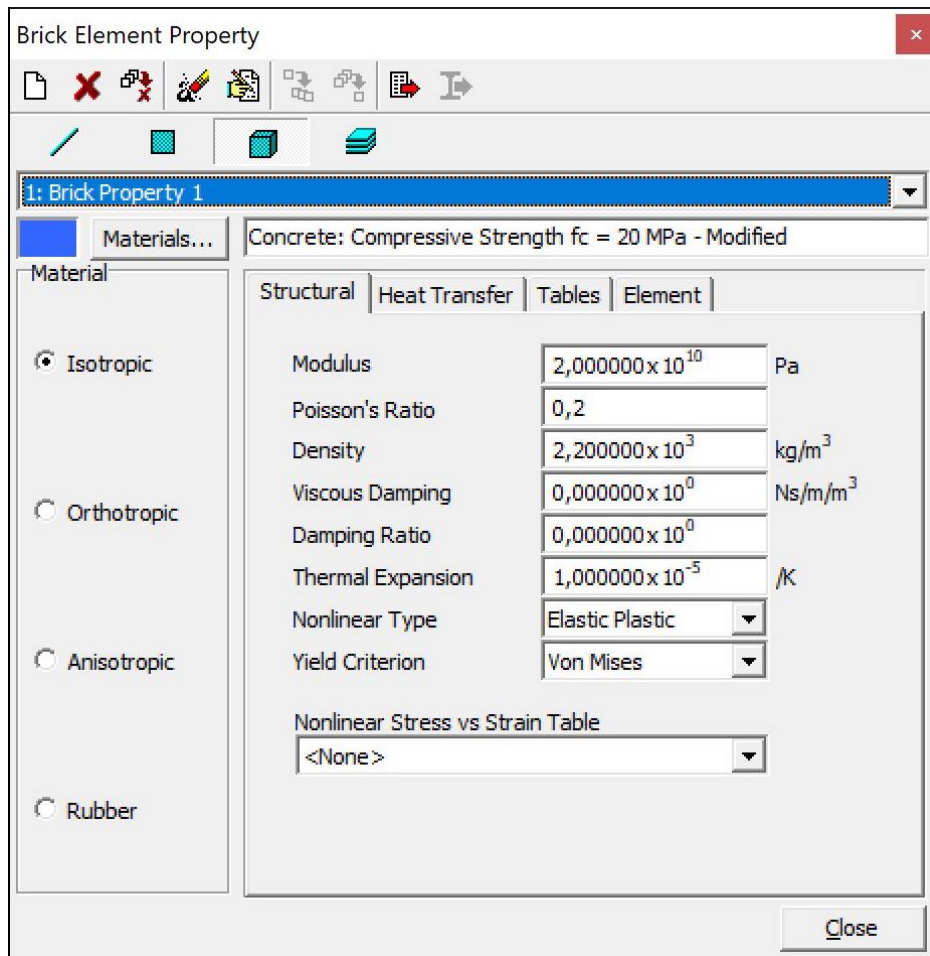


Figure 35 – Material property's dialog box containing the selected options

The material property just defined was then applied to all the bricks composing the segment model. At this stage, to further proceed with the analysis, virtual constraints had to be set so that they were able to reproduce the best the apparent results of the interaction between the San Lorenzo tunnel and the landslide body inside which it is located. In the paper called “*Structural health monitoring of a road tunnel intersecting a large and active landslide*”, the authors Bossi and Marcato (2017), by analyzing and interpreting the data collected from the road tunnel monitoring system, have suggested that the 28th segment was constrained to the stable slope on the left, while it was stressed by the landslide induced movements on the right, consequently working as a loaded cantilever. As an additional consideration looking at the two adjacent segments, cracks orientation and widening suggested that the 27th segment has taken advantage of the independent segments design solution and has undergone roto-translation.

On the other hand, the 29th segment seemed to be mostly located at the stable region, with the crackmeters showing negligible displacements (Fig. 36).

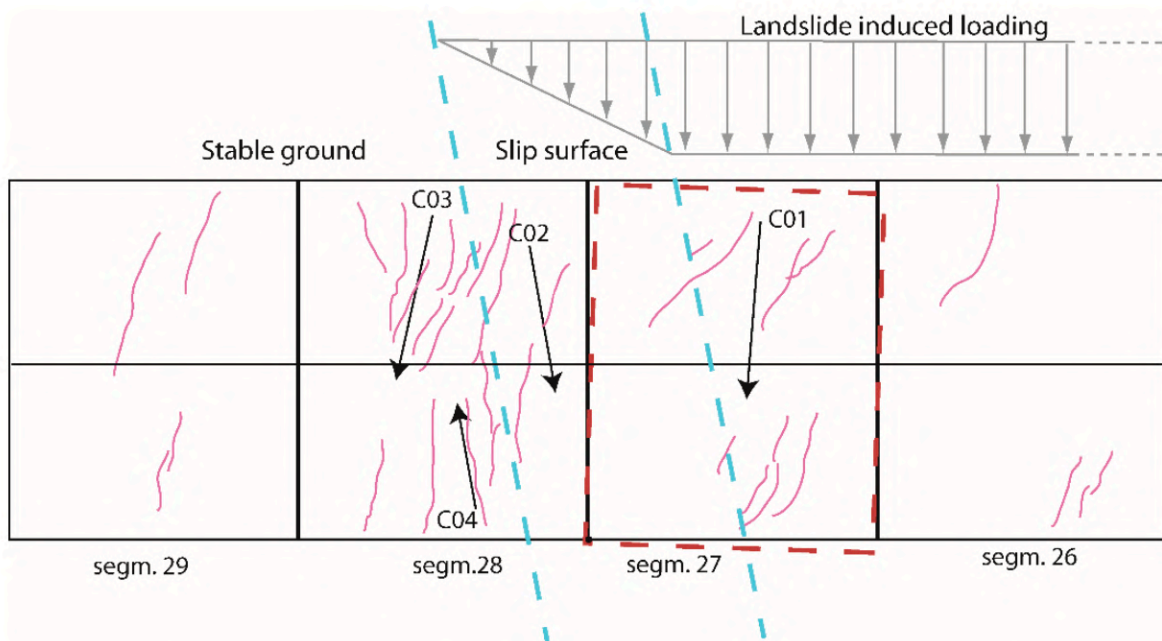


Figure 36 – Suggested loading scheme and road tunnel response (Bossi, G., Marcato, G., 2017)

With respect to the observations described above and the fact that the so far modeled segment must reproduce the 28th segment behavior, as first trial all the nodes on both front and back cross-sections have been constrained in a way that they behave as a unique infinitely rigid mean. To practically make so, Straus7 provides a tool called *Link*, with many different options regarding the offered property and functionality. After several attempts and related speculations, among the available options, the rigid link has been selected since it has proved to fulfill most of the characteristics required to the constraints.

In the Straus7 environment, a rigid link between two nodes is used to represent a rigid bar connecting them. By providing restraints to nodal rotations and to translational displacements, it can be compared more to a very stiff beam element rather than a very stiff element. A rigid link may act in one of the global coordinate planes or in general 3D space, depending on the plane option selected (XY, YZ, ZX, XYZ). Rigid links are typically used to model, for instance, rigid diaphragms for the analysis of floor slabs. Continuing with this example, to reproduce the assumption of a floor slab lying in the XY plane to be infinitely rigid

against in-plane loads, rigid links can be used between the nodes in the XY plane. Out-of-plane displacements are not constrained by these links, letting the floor slab to deflect laterally, with the projection of the deflected slab onto the XY-plane showing a rigid movement without in-plane deformation.

Resuming to the FEM model of the San Lorenzo tunnel's segment, rigid links with the XYZ plane option selected have been applied to the front and back cross-section, so that all the nodes belonging to those sections were linked to the center of gravity of the respective section and behaved as a unique infinitely rigid object in the 3D space, as it is shown in the figure below (*Fig. 37*).

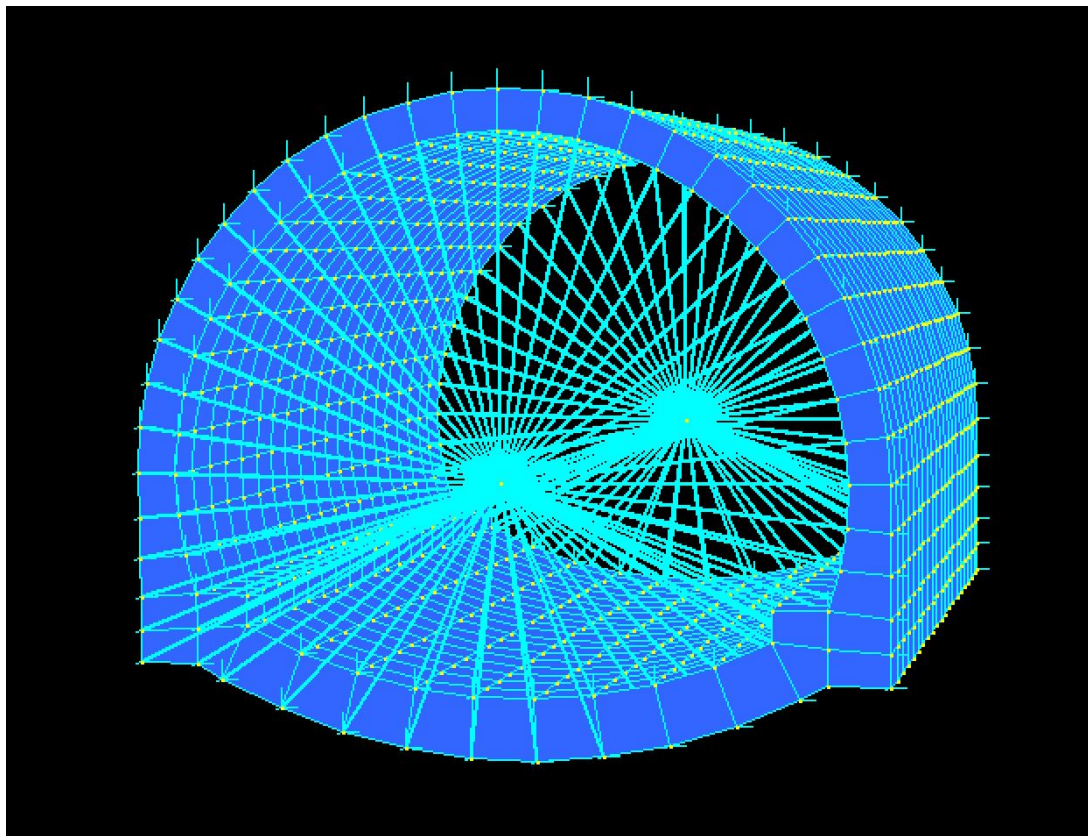


Figure 37 – San Lorenzo tunnel single segment mesh with rigid links applied on both front and back cross-sections

The use of rigid link allows one to apply any force or deformation directly to any node belonging to the infinitely rigid object at hand and obtain as result its uniform application on the entire object. Given that the construction of the model has reached the development of a random San Lorenzo tunnel's segment with an adequate similarity with the real one, the applications of some basic situations

have been carried out to preliminarily test the aforesaid model. Specifically, keeping one of the closing cross-sections fixed, three simple movements have been directly applied on the center of gravity of the free-to-move cross-section:

- 10 cm displacement in X direction (*Fig. 38*);

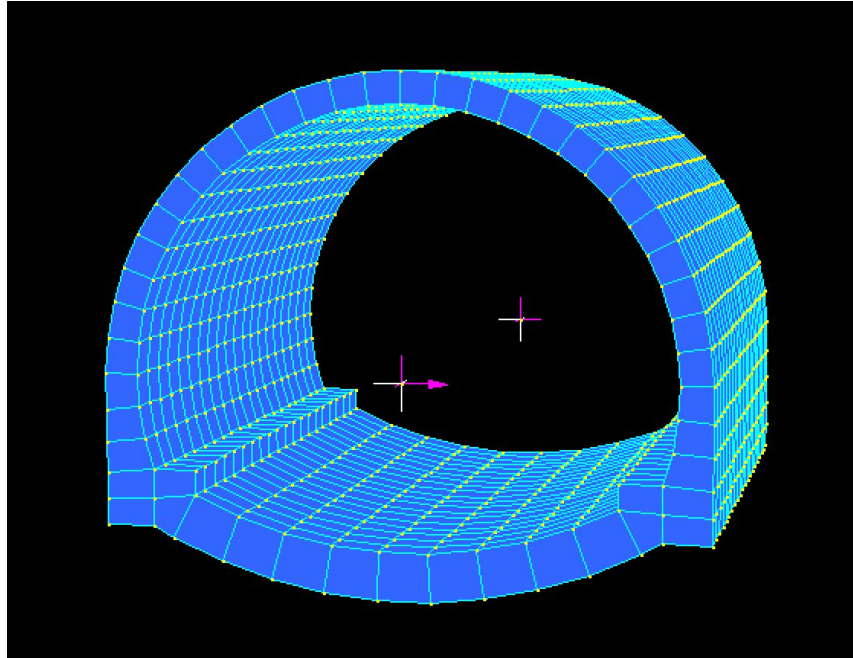


Figure 38 – San Lorenzo tunnel single segment mesh with 10 cm displacement applied in X direction

- 10 cm displacement in Y direction (*Fig. 39*);

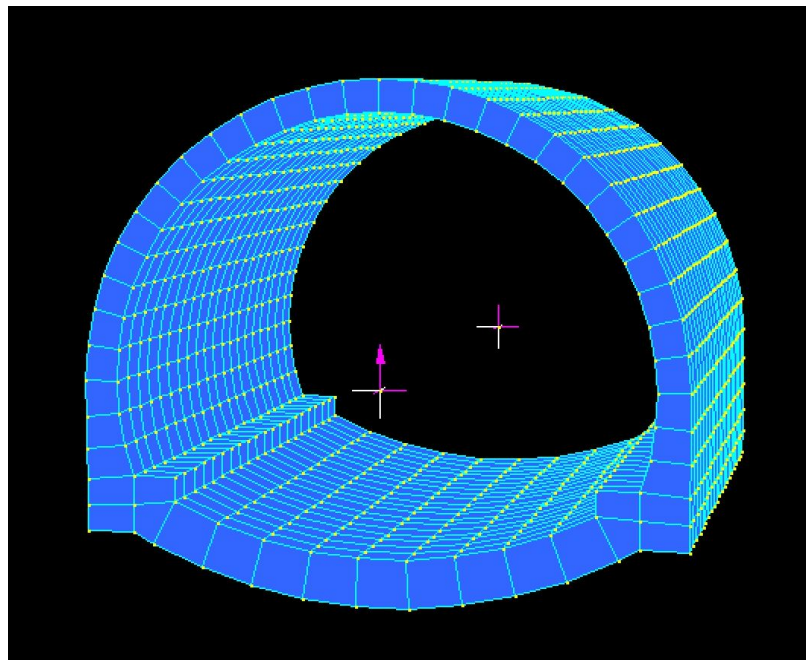


Figure 39 – San Lorenzo tunnel single segment mesh with 10 cm displacement applied in Y direction

- 10° rotation around X axis (*Fig. 40*).

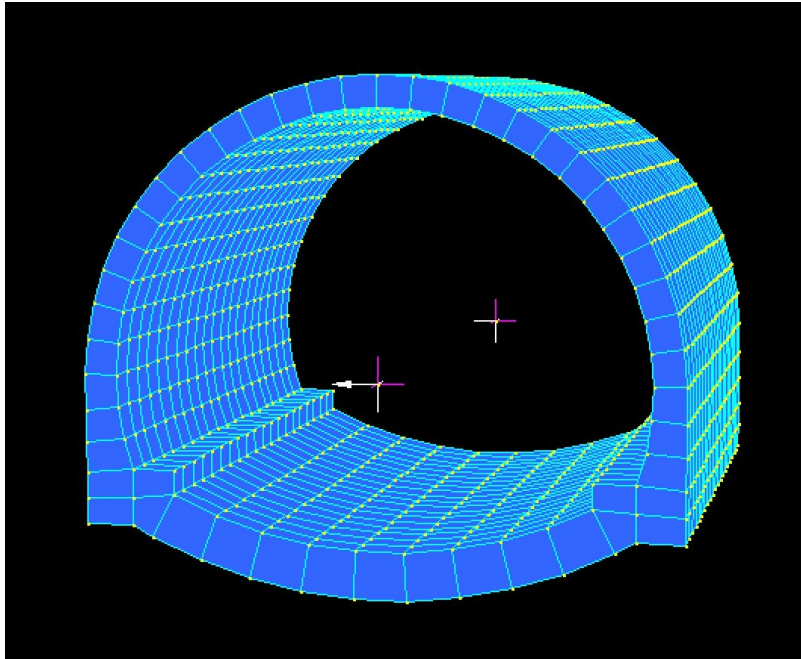


Figure 40 – San Lorenzo tunnel single segment mesh with 10° rotation applied around X axis

In the following table the outcoming results of this first trial in terms of stress distribution are graphically reported through the contour visualization option provided by Straus7. Only the table related to the 10 cm displacement in X direction has been shown, since the purpose was just to expose few of the preliminary results reached.

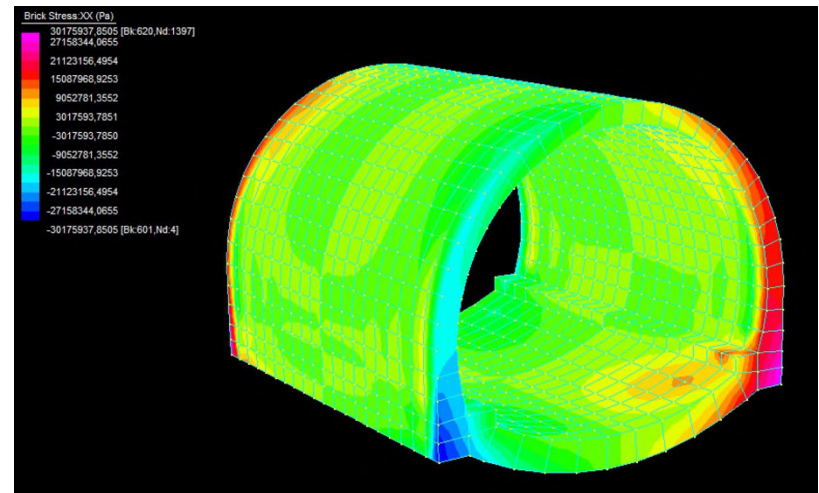
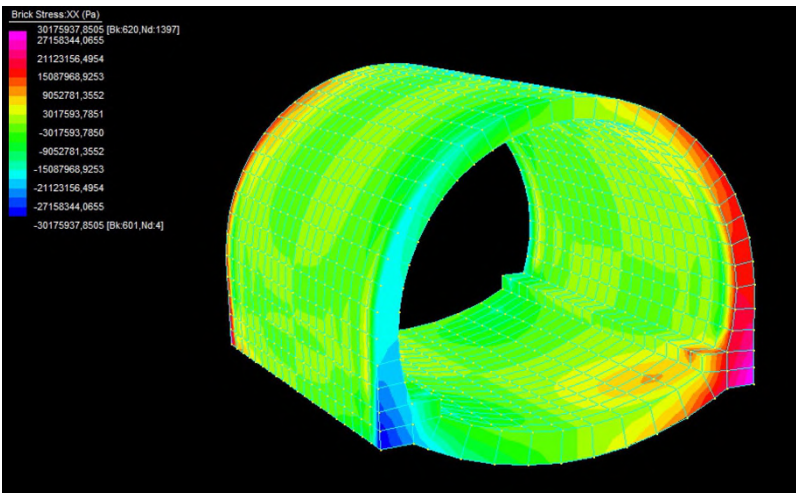
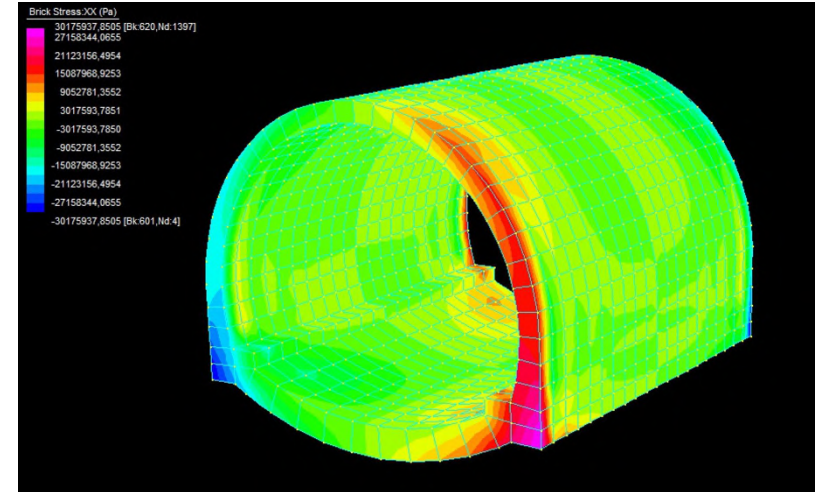
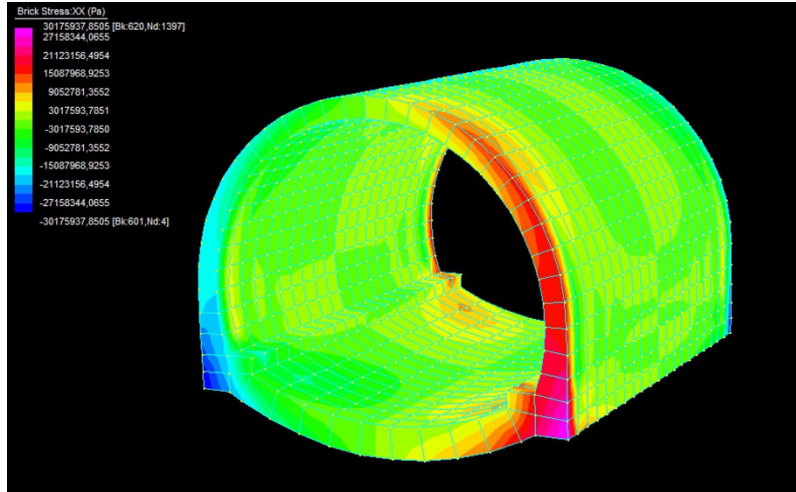
10 cm DISPLACEMENT IN X DIRECTION

Straus7
contour
visualization
option

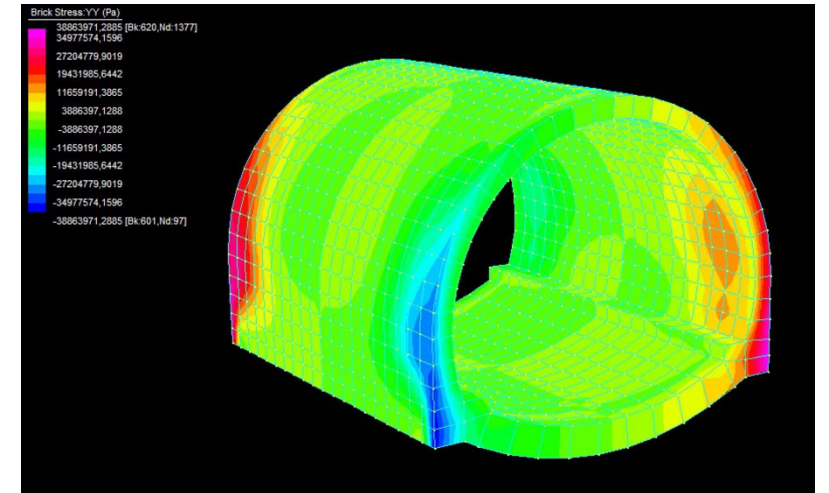
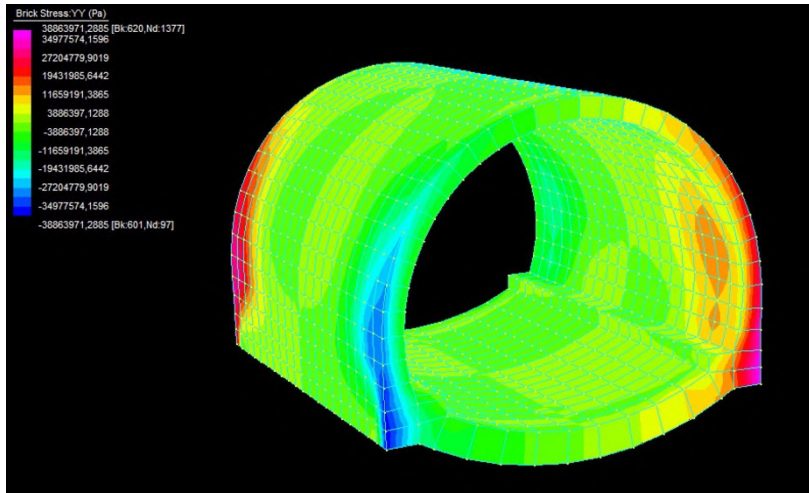
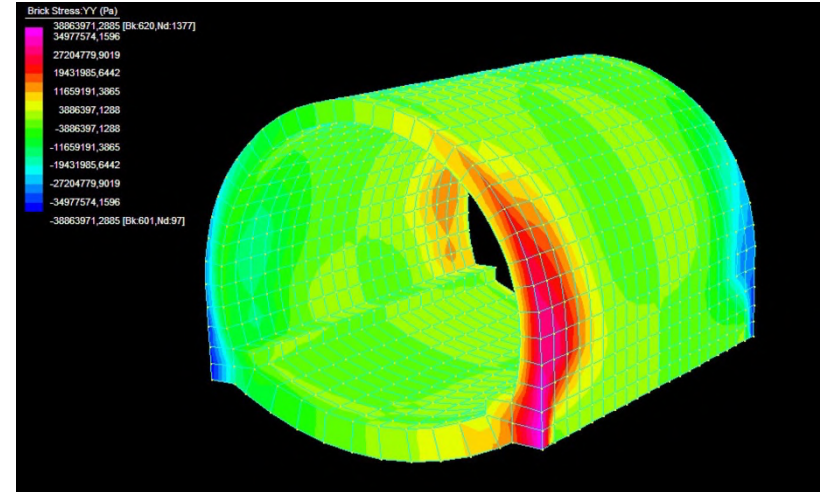
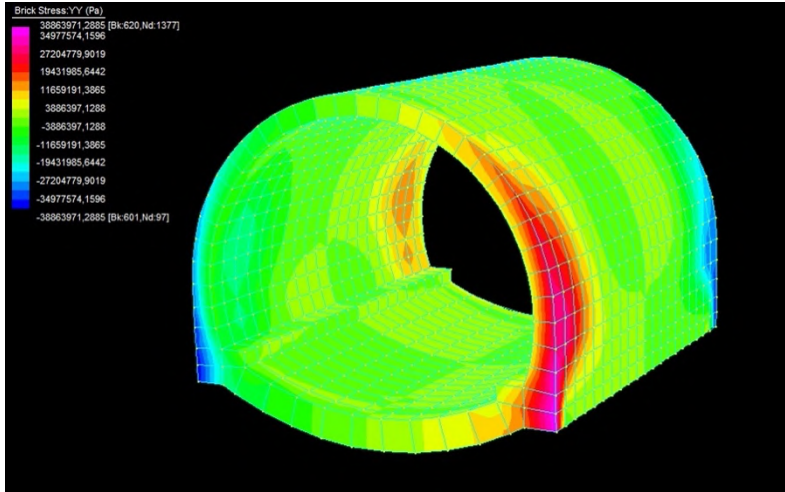
Constrained section foreground

Fixed section foreground

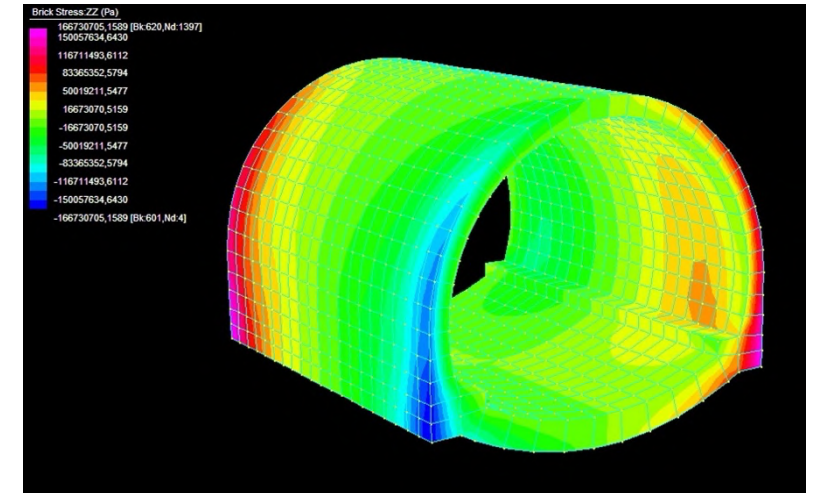
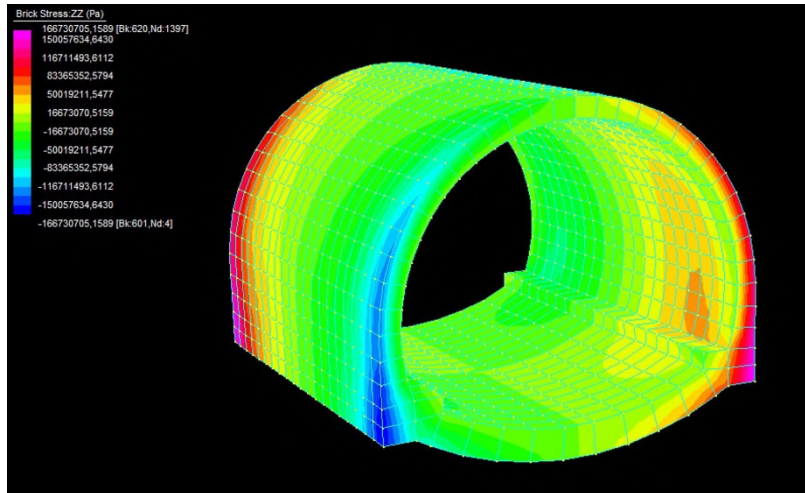
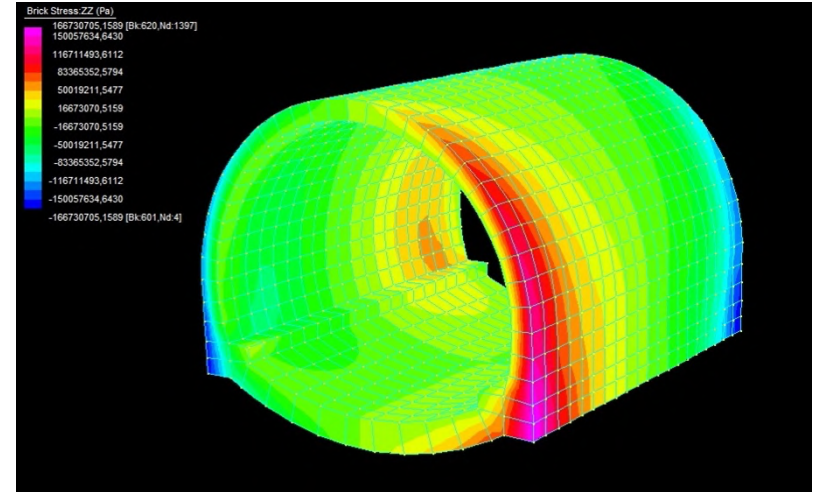
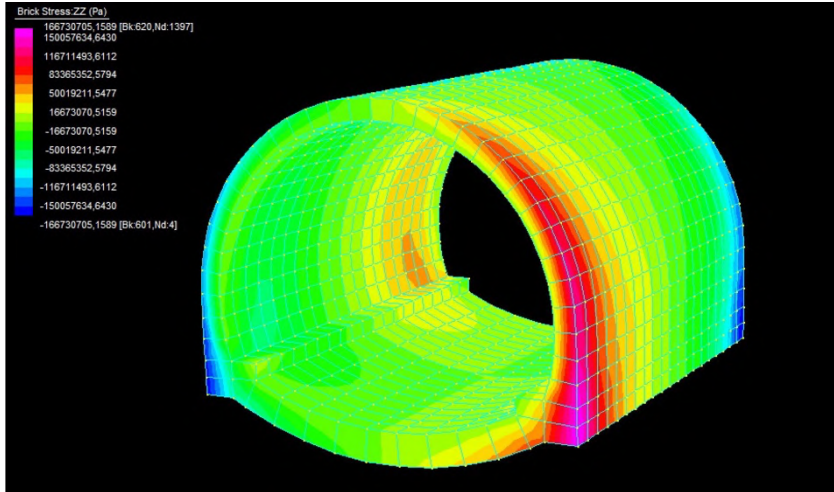
XX



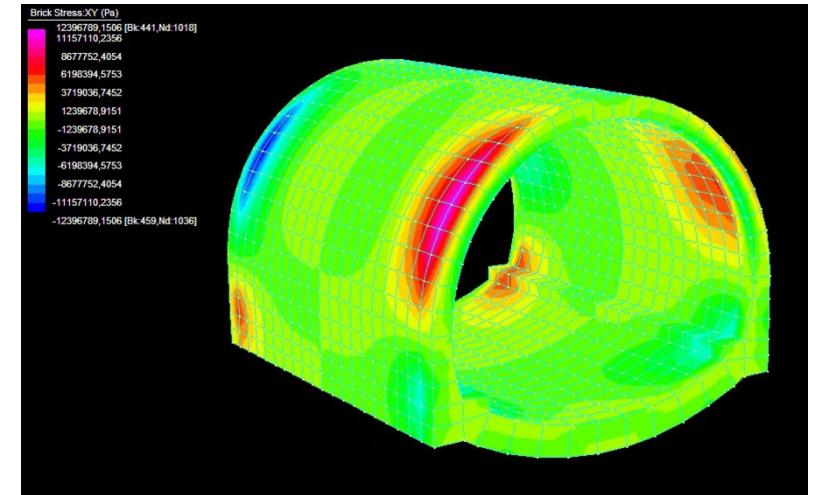
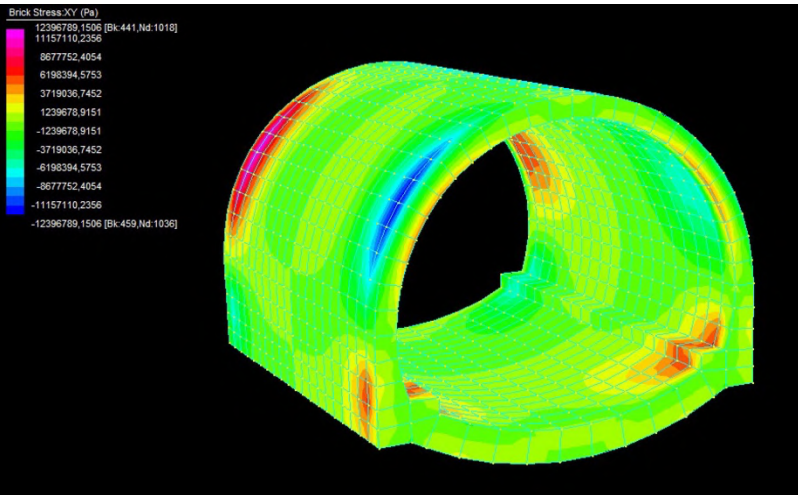
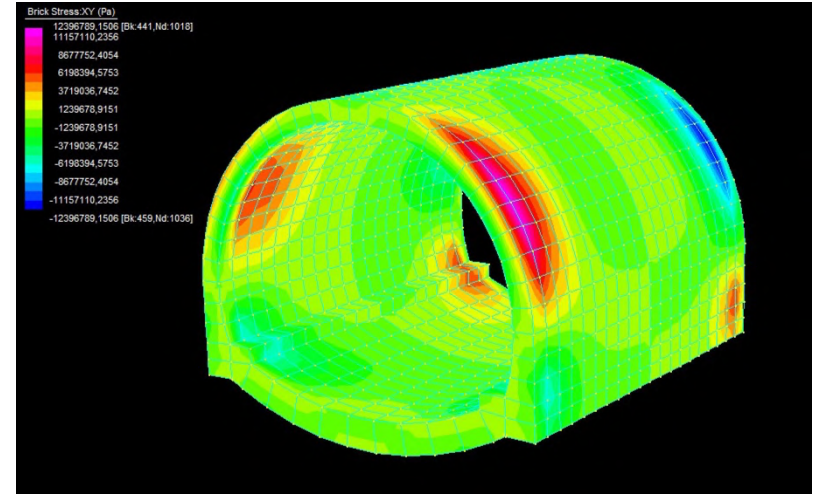
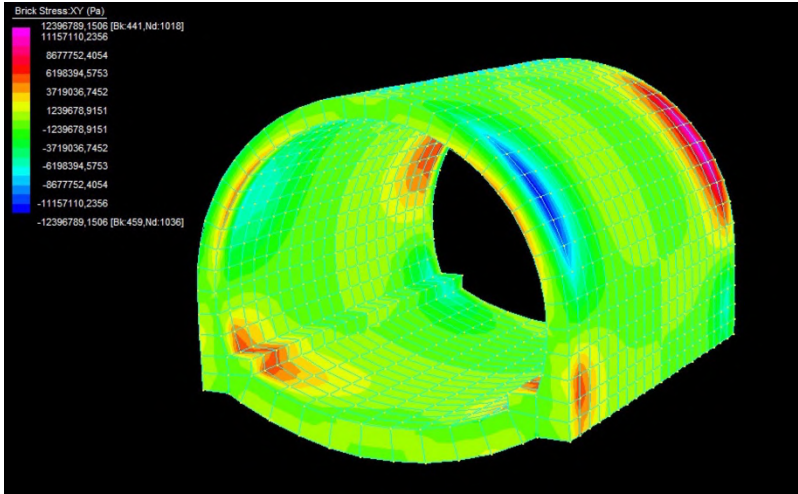
YY



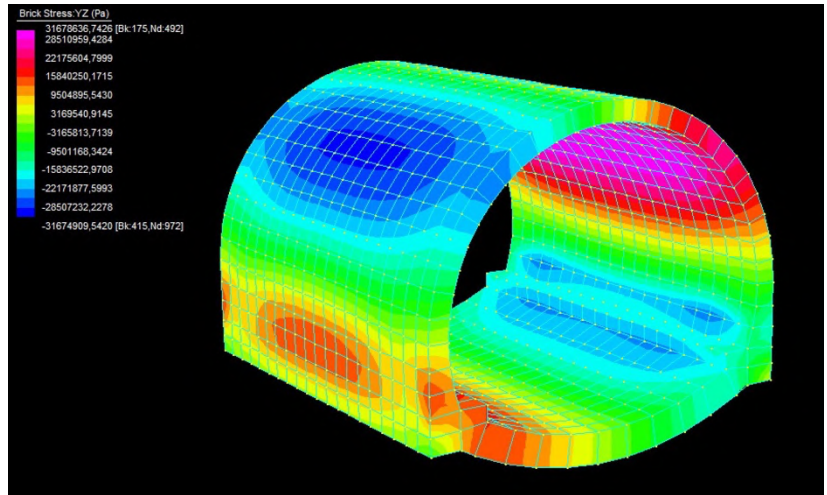
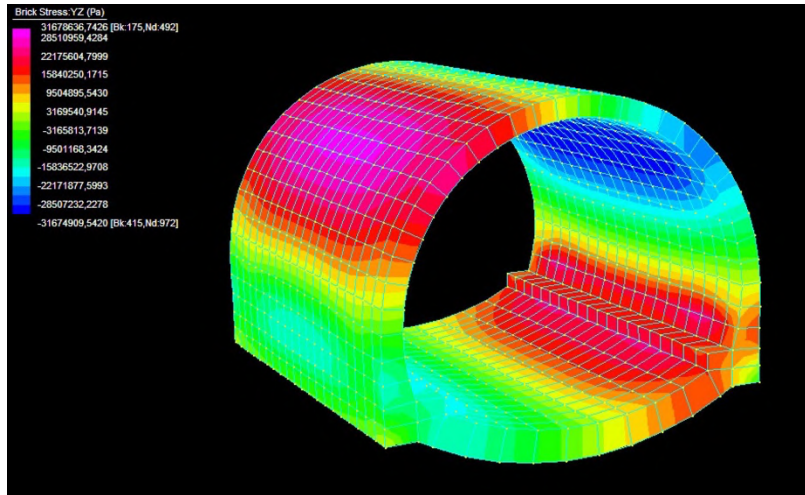
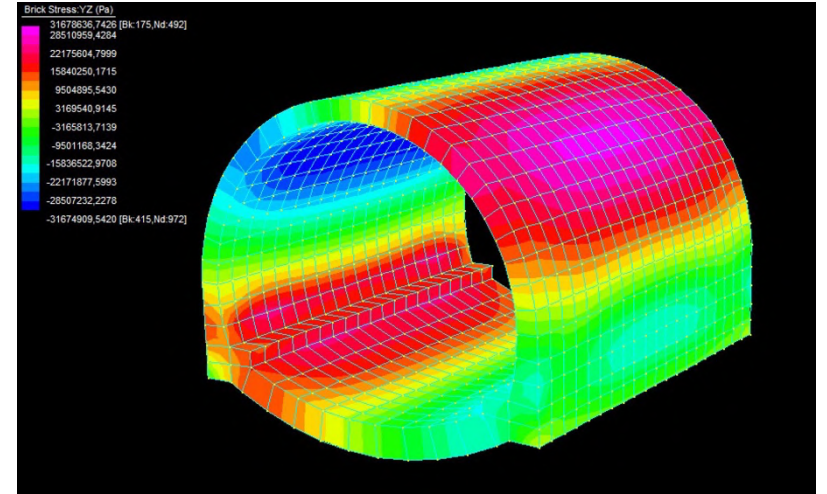
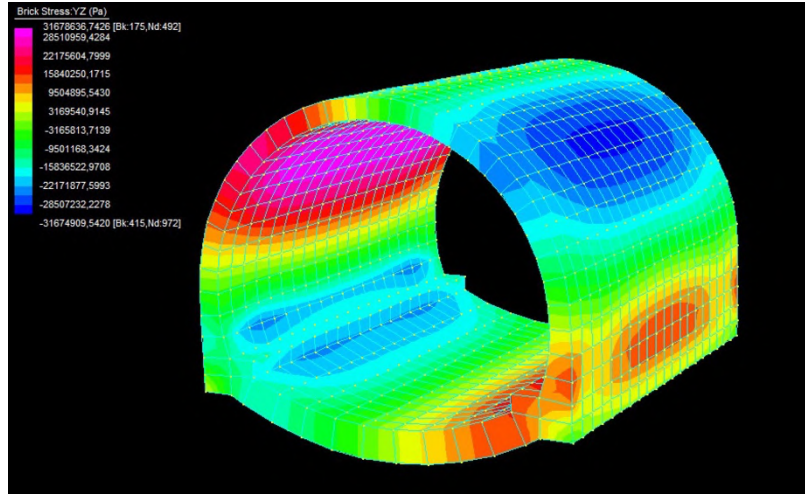
ZZ



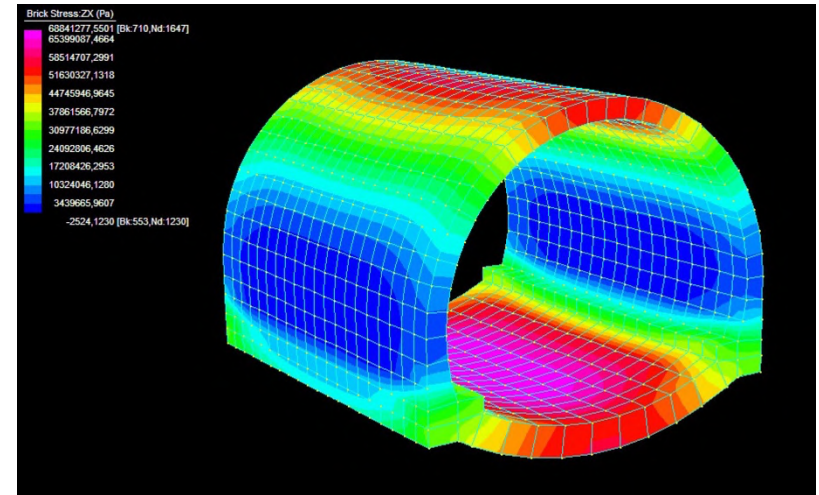
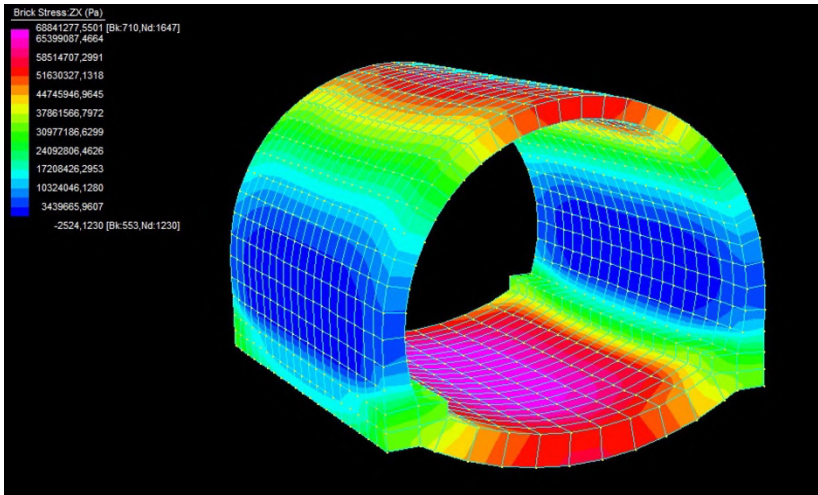
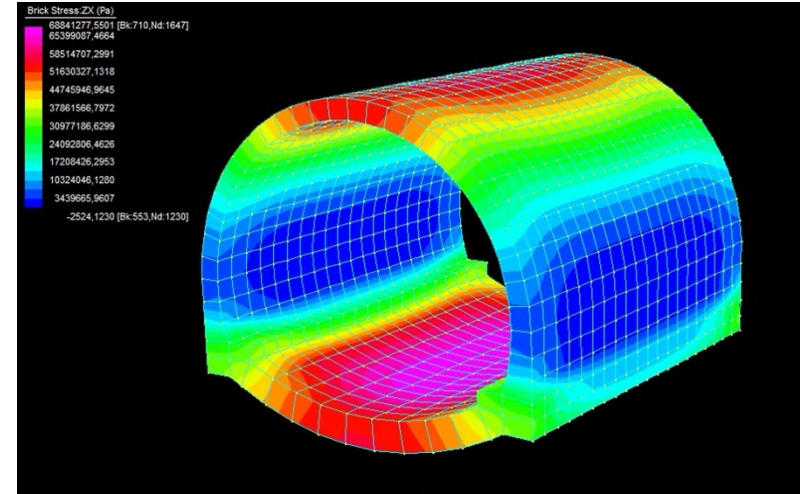
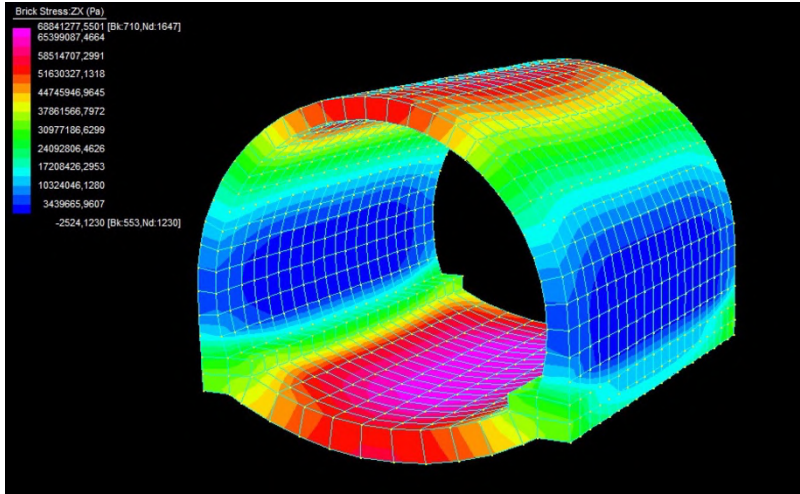
XY



YZ



ZX



As previously described in detail, Straus7 proceeds in determining the elements stress, strain and nodal reactions by solving the general equilibrium equations. Thereafter, the software allows the user to visualize the obtained results in many distinct ways, depending on what needs to be highlighted. In this phase of the San Lorenzo road tunnel modeling, the contour visualization of stresses option was deemed as the most relevant and representative one in order to search confirmation of the choices made so far.

To help navigate in the results presented in the table, the used symbology needs to be explained. The letters contained in the first column stand for the type of stress depicted in the nearby figures. This notation is based on defining the cut plane in which the force is acting, expressed with the first subscript, and the direction the force is acting in, indicated by the second subscript (*Fig. 41, 42*).

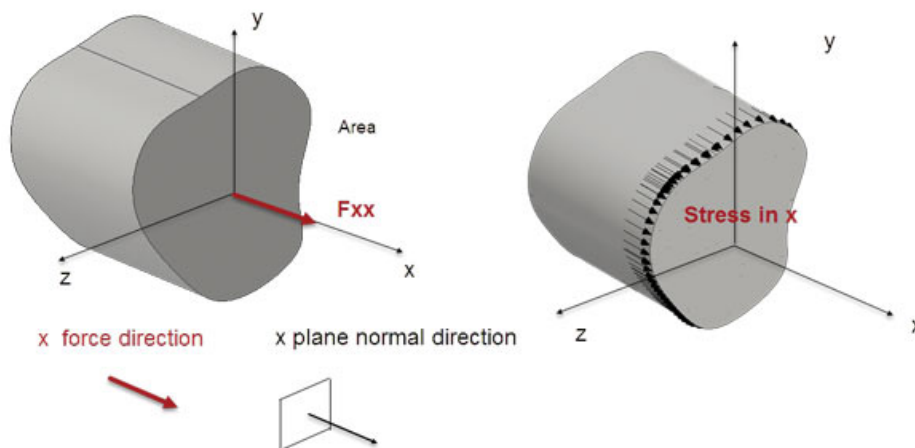


Figure 41 – Normal force and stress in X direction and X normal plane (G+D Computing Pty Limited, 2004)

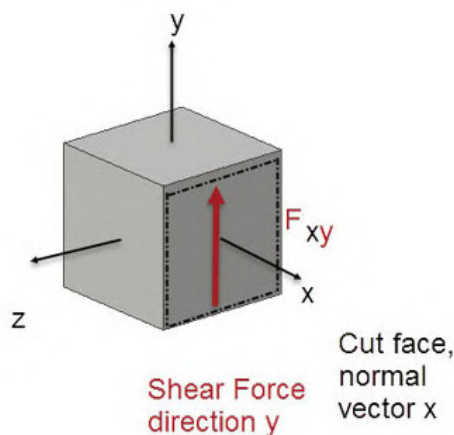


Figure 42 – Shear force in Y direction and X normal plane (G+D Computing Pty Limited, 2004)

Since a stress can be seen as the measure of the intensity of a force per unit area, S_{xx} , S_{yy} and S_{zz} are the stresses acting normal to the respective cut faces, also known as normal stresses, while S_{xy} , S_{yz} and S_{zx} are the so-called shear stresses (Fig. 43). In the first column of the table, for sake of simplicity, only the subscripts of those stresses are reported.

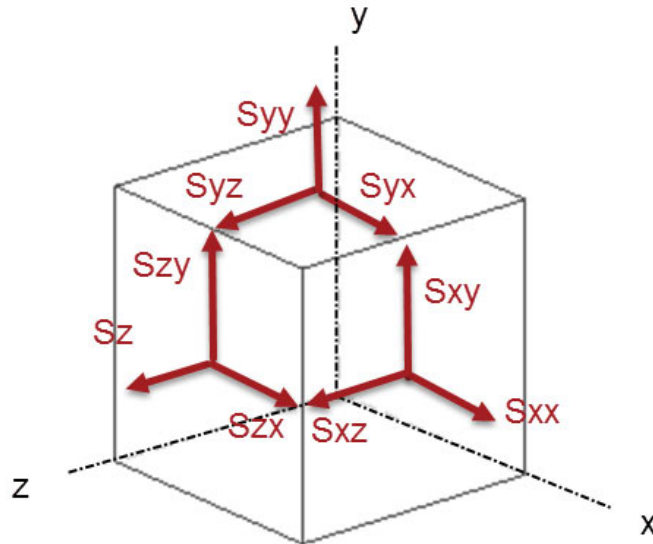


Figure 43 – Representation of both normal and shear stresses on visible faces (G+D Computing Pty Limited, 2004)

In the second and third columns, the outcoming stresses' distributions have been divided with respect to the cross-section portrayed foreground and displayed using a color gradient, which gives an immediate picture of the overall trend. Specifically, elements of the structure depicted in reddish colors are characterized by compression, while the ones depicted in blueish colors are characterized by tension.

By looking at the obtained outcomes some considerations have arisen. Firstly, no stress distribution directly and strongly relatable to the occurrence of the detected fractures on the vault has been found. In the second place, the, in a way, imposed by the applied constraints and hypothesized cantilever behavior has not been reflected in any of the cases in the table. Indeed, the only mild evidence of a cantilever performance might be attributed to the compressed and strained fibers' alternance, noticeable on the outermost portions of the closing sections in the normal stresses' cases (XX, YY and ZZ). This latter remark led, lastly, to a final consideration, which claimed an involvement of the so-called

board effect in the concentration of stresses on the closing portions of the modeled segment. Anomalies or peculiar behaviors in terms of forces located on the extremities of objects or spaces are often related to the impact of this effect. To better investigate the effective influence of the board effect, the analysis has been run again, adding two more segments in front and behind the one already modeled, keeping constrained by the network of rigid links the ending cross-sections of each of the three segments (*Fig. 44*).

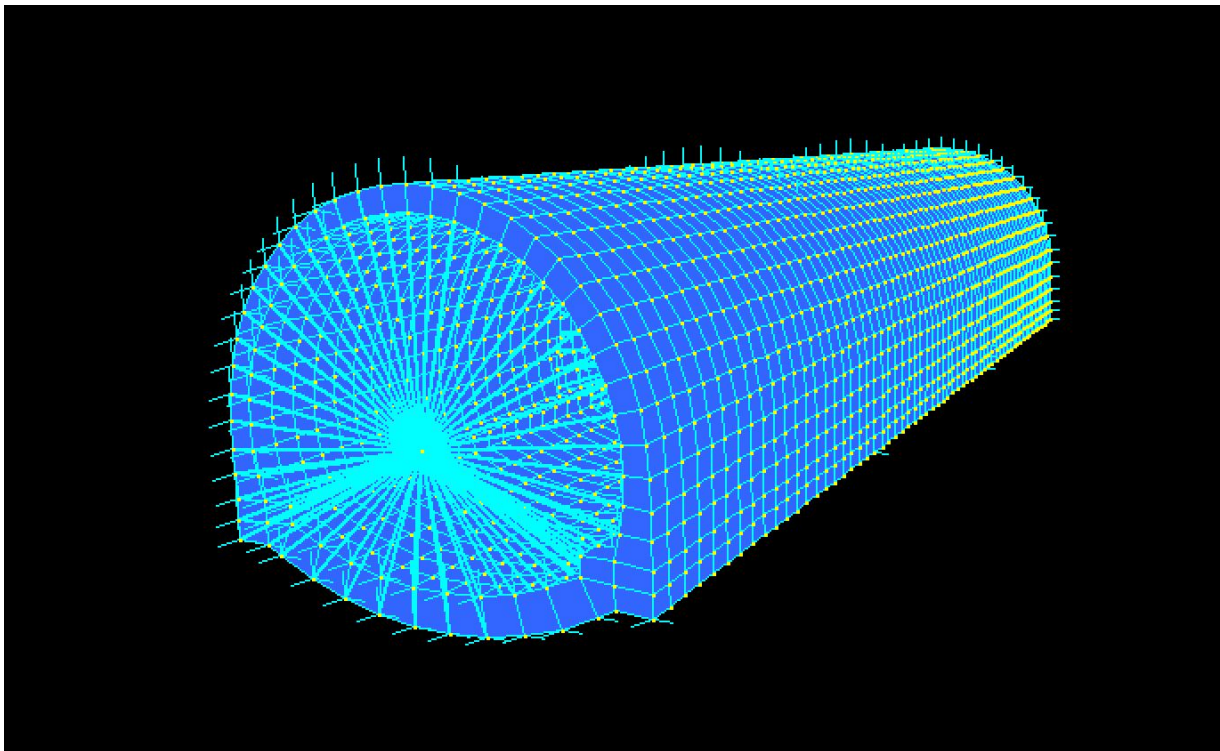
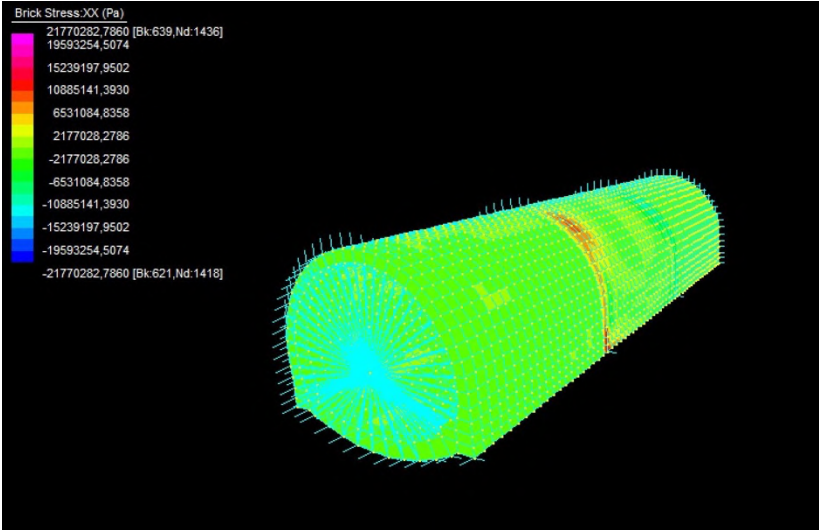
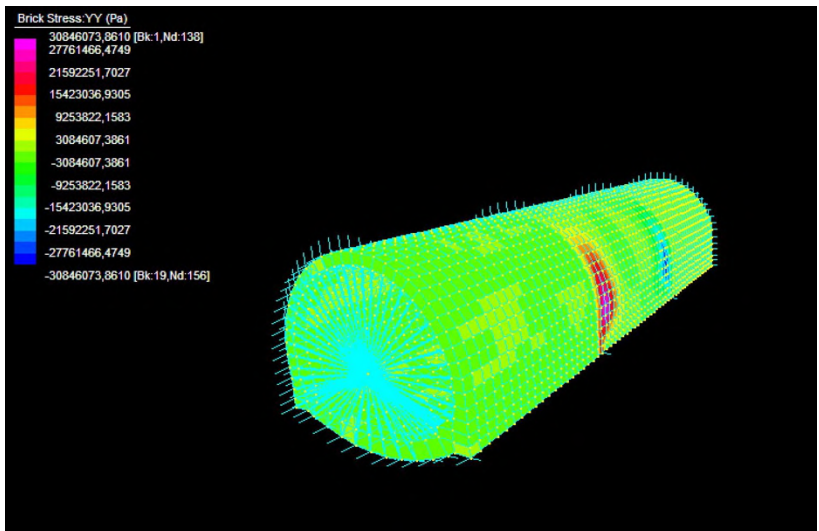
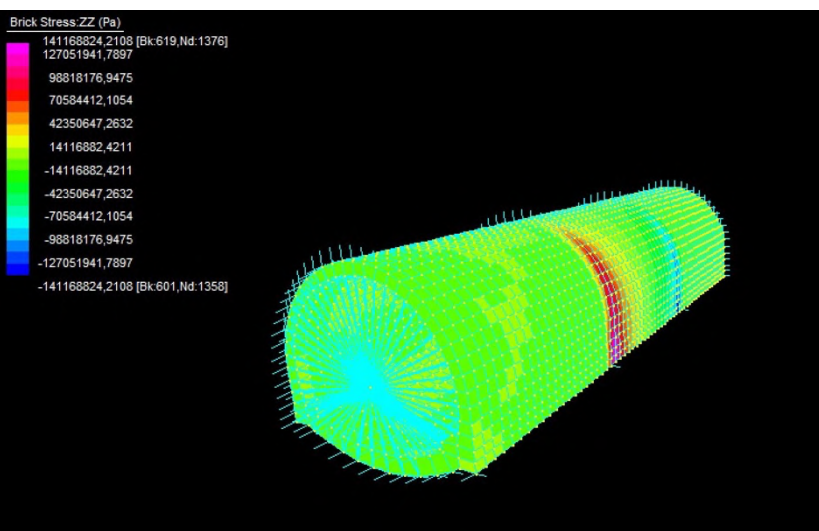


Figure 44 – San Lorenzo tunnel mesh comprising three segments

The obtained results have shown a light dissipation of the aforesaid effect, confirming its influence, although eventually negligible, on the global stresses' trend.

Straus7 contour visualization option	Constrained section foreground
XX	 <p>Brick Stress:XX (Pa)</p> <ul style="list-style-type: none"> 21770282,7860 [Bk:639,Nd:1436] 19593254,5074 15239197,9502 10885141,3930 6531084,8358 2177028,2786 -2177028,2786 -6531084,8358 -10885141,3930 -15239197,9502 -19593254,5074 -21770282,7860 [Bk:621,Nd:1418]
YY	 <p>Brick Stress:YY (Pa)</p> <ul style="list-style-type: none"> 30846073,8610 [Bk:1,Nd:138] 27761466,4749 21592251,7027 15423036,9305 9253822,1583 3084607,3861 -3084607,3861 -9253822,1583 -15423036,9305 -21592251,7027 -27761466,4749 -30846073,8610 [Bk:19,Nd:156]
ZZ	 <p>Brick Stress:ZZ (Pa)</p> <ul style="list-style-type: none"> 141168824,2108 [Bk:619,Nd:1376] 127051941,7897 98818176,9475 70584412,1054 42350647,2632 14116882,4211 -14116882,4211 -42350647,2632 -70584412,1054 -98818176,9475 -127051941,7897 -141168824,2108 [Bk:601,Nd:1358]

The first two considerations previously done, though, were still not justified or deepened. Resuming to the single element kind of model, a supplementary examination on the reasons behind the absence of a coherent congruence between the observed concrete lining's damages and the resulting stress outputs has been undertaken, starting from a new interpretation of the road tunnel behavior hypothesized by Bossi and Marcato (2017), shown in Figure 36. Here, indeed, the landslide-induced load is reported as a pressure with a triangular increasing trend, applied on a specific portion of the segment. Hence, thanks to a Straus7-provided option for bricks named *Face press* → *Global* (Fig. 45), a X-directed face pressure of a random value has been applied, but not on the entire segment, instead just on the half of it, and on half of the upper vault, completely excluding the lower one and the internal sidewalk portion. Keeping unchanged the constraints' setting, this latter disposal has been arranged as shown in the figures below (Figg. 46, 47).

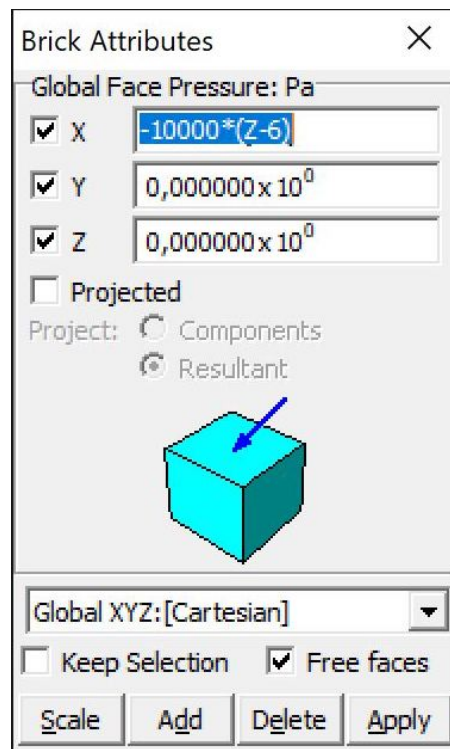


Figure 45 – Face press dialog box

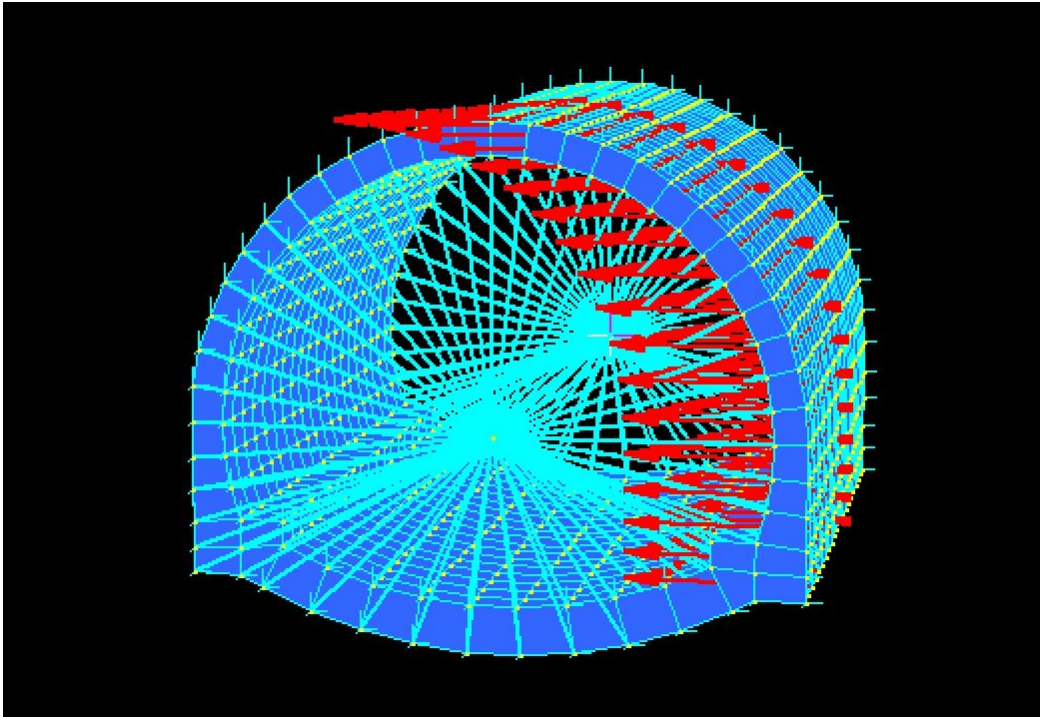


Figure 46 – San Lorenzo tunnel mesh under triangular trend face pressure loading and rigid link network on both closing cross-sections

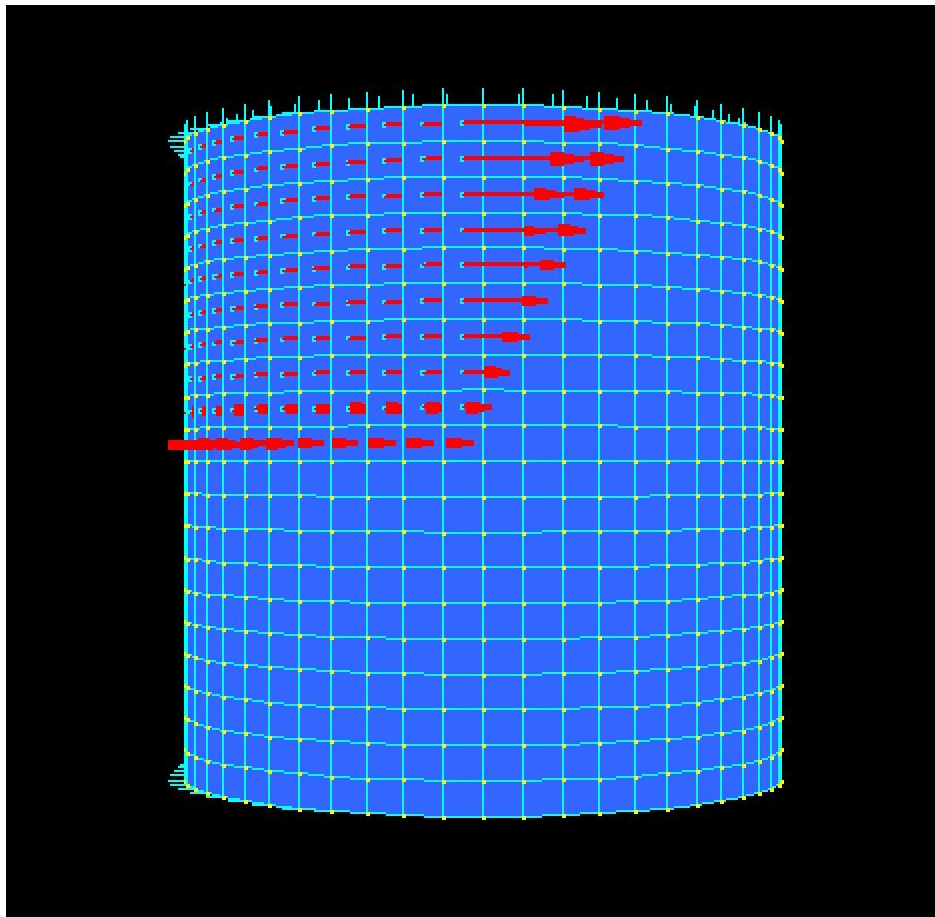


Figure 47 – Above view of San Lorenzo tunnel mesh under triangular trend face pressure loading and rigid link network on both closing cross-sections

By looking at the outcomes of the above modelled scenario, evidence of the formerly exposed second consideration could be found too. As a matter of fact, the global deformation, presented in the figure below (*Fig. 48*), thanks to the dedicated Straus7 option which enables to observe the foreseeable structure's deformations under the imposed loads or displacements, differed from the cantilever's expected and designed one, as the segment looked like it has been pressed mostly in the portion where it has been charged, recalling a metallic-can-like performance.

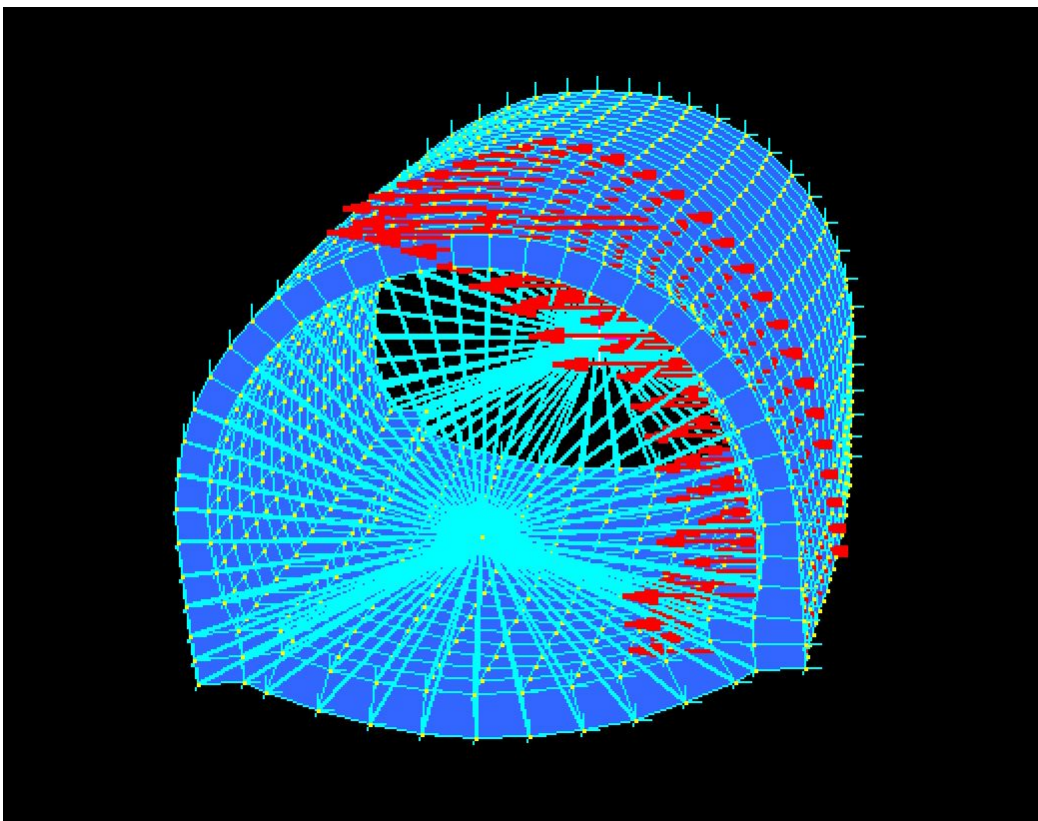


Figure 48 – Deformed San Lorenzo tunnel mesh under triangular trend face pressure loading and rigid link network on both closing cross-sections

To enhance even more the discarding of this latter San Lorenzo tunnel's model, the outcoming stresses' results have revealed an abnormal distribution, distant from the one relatable to a cantilever behavior and to the one linkable to the concrete fractures onset too. The highest stresses have been indeed localized at the right corresponding height, but poorly spread on the vault's surface and with values not high enough to create actual damages. (*Fig. 49*).

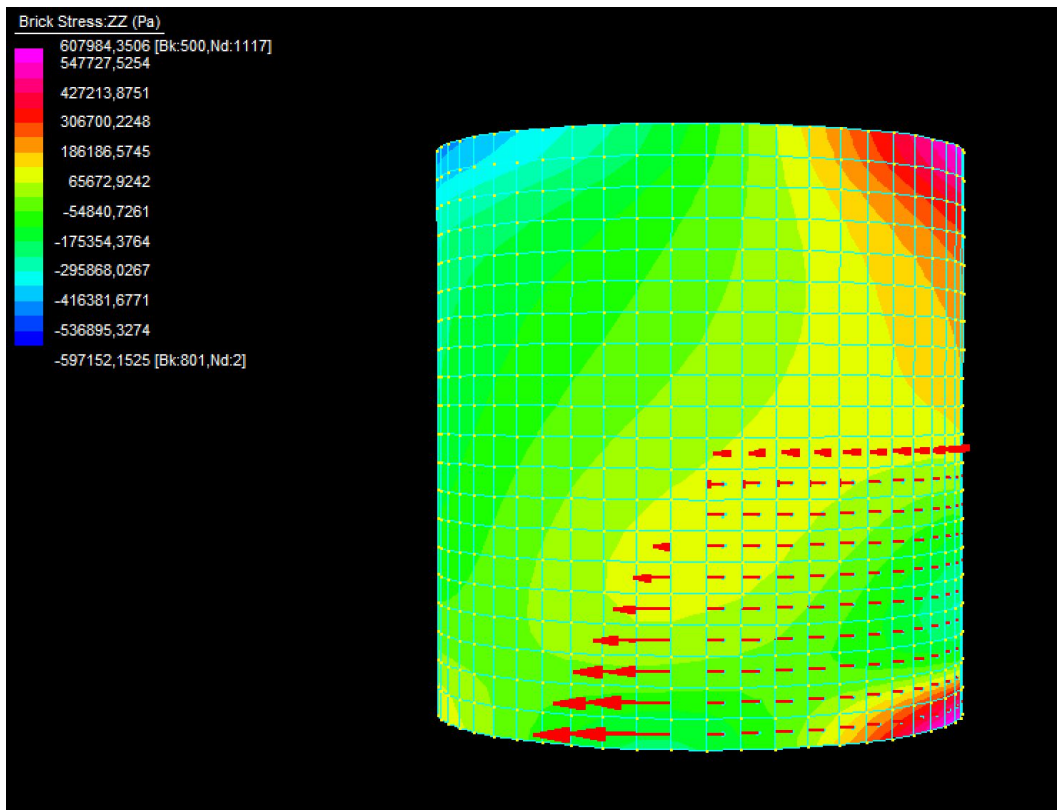


Figure 49 –San Lorenzo tunnel stress distribution along the Z direction under triangular trend face pressure loading and rigid link network on both closing cross-sections

Given that the results obtained so far have shown neither relevant nor clear evidence of the earlier cantilever behavior hypothesis, the trial-and-error procedure has been urged to continue with new considerations and developments.

At this point, the reasoning carried on has been focused on the network of rigid links applied on the ending sections. So, instead of constraining the assessed as free-to-move cross-section, the latter has been released from the rigid links. In fact, the rigid links' network applied in this section has been deemed as responsible for disabling a proper cantilever behavior. The network on the other section, instead, has been kept, as well as the fixed conditions applied to it. The loading enacted by the triangular increasing trend global pressure on the earlier described portion of the segment was maintained too. This latter arrangement has been shown in the figures below (*Figg. 50, 51*).

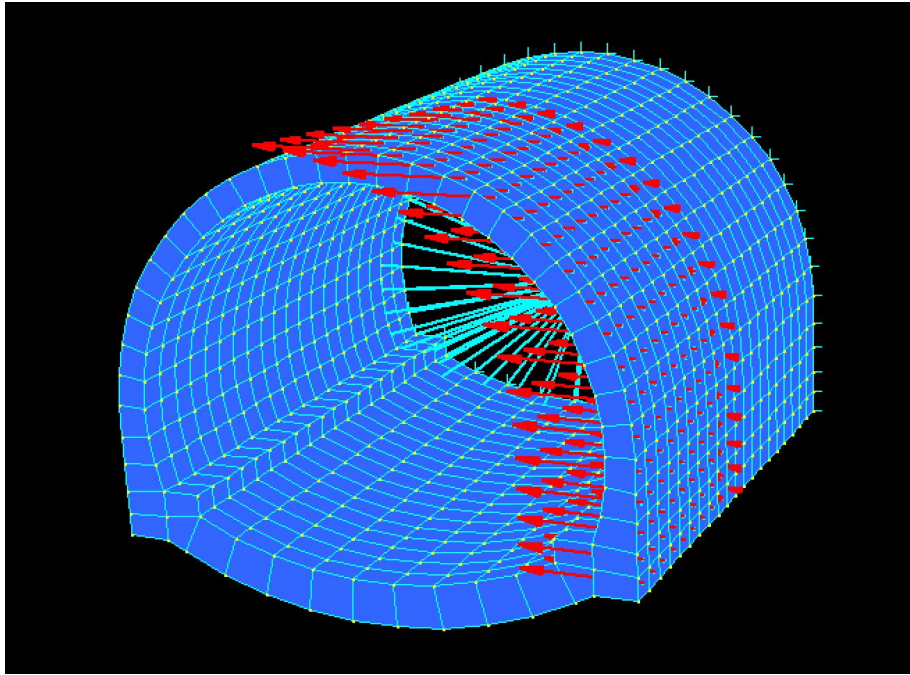


Figure 50 – San Lorenzo tunnel mesh under triangular trend face pressure loading with a constraints-free cross-section

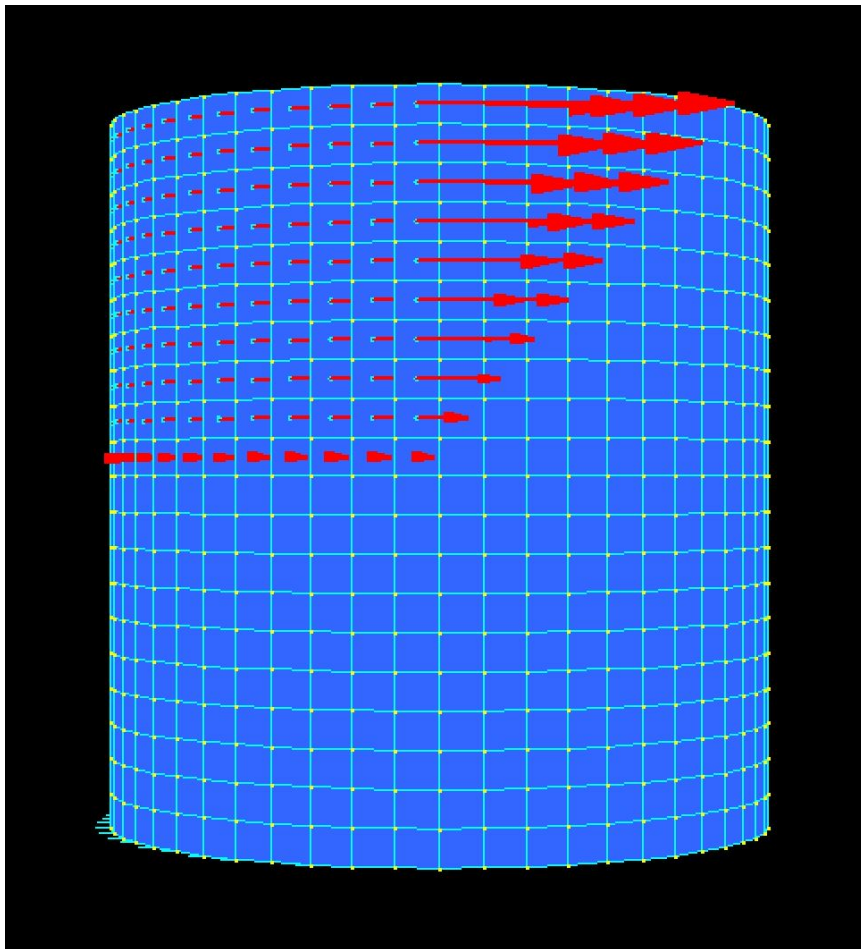


Figure 51 – Above view of San Lorenzo tunnel mesh with triangular trend face pressure loading constraints-free cross-section

From the outcoming ultimate results it might be said that the cantilever behavior is barely confirmed. As a matter of fact, *thanks to the dedicate Straus7 option which enables to observe the foreseeable structure's deformations under the imposed loads or displacements*, the segment has appeared to undergo deformations relatable to a cantilever performance, as it can be seen in the following figure (*Fig. 52*).

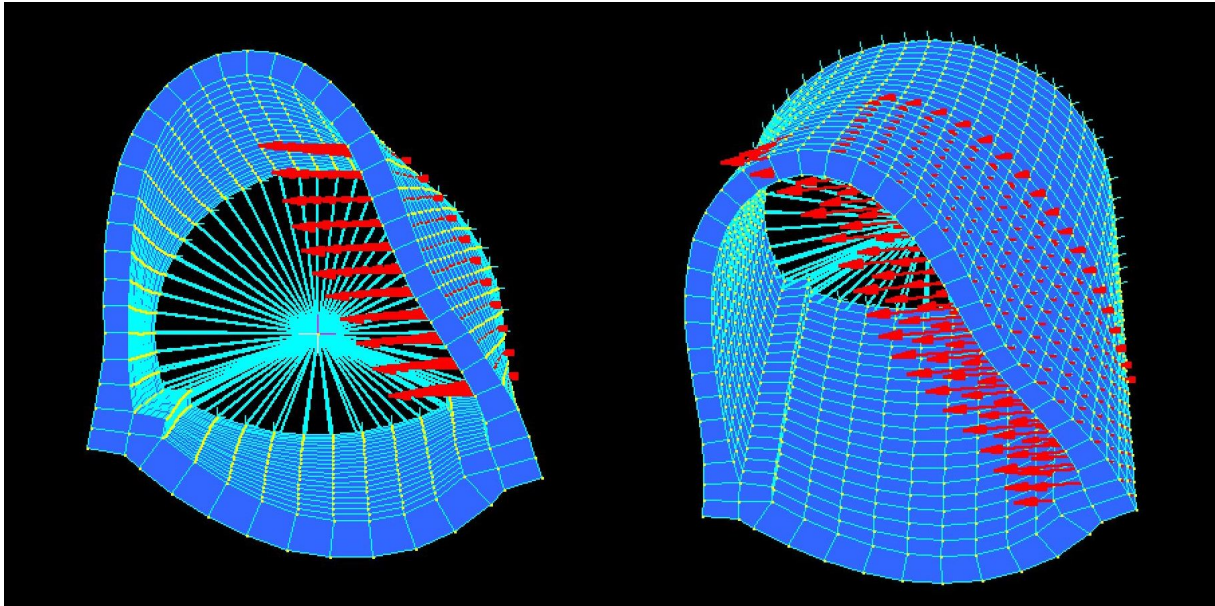


Figure 52 – Views of the deformed San Lorenzo tunnel mesh with triangular trend face pressure loading

As a further validation of the comment above on the deformed state of the modeled segment, also the stress distribution kind of results showed a cantilever behavior, through an alternance of the compressed and strained fibers similar to the one already detected in the opening trial. In terms of stress's spreading and contingent cracks' spots, the same considerations made for the previous model attempt could be done. It is clearly needed a deepening on this specific topic, looking for answers (*Fig. 53*).

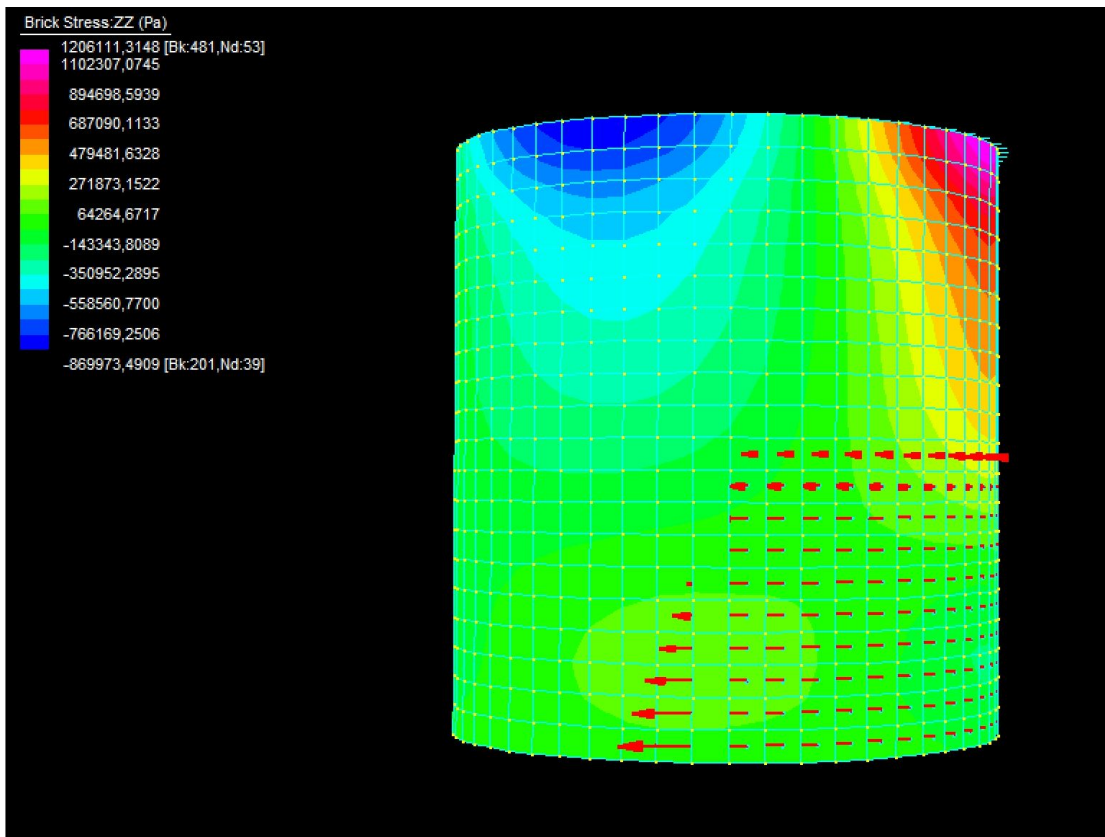


Figure 53 –San Lorenzo tunnel stress distribution along the Z direction

Conclusions

This work represents the first step towards the objective of tracing back the sum of landslide-induced stresses and forces, which are directly responsible for the actual cracks' pattern, visible on the most damaged segments of the San Lorenzo road tunnel, especially on the 28th one.

The exhibited workflow of this dissertation is dense and articulated and starts from solid observations to enable a reasonable modeling process. Thinking of this work as divided into two phases, the first one brought the creation of a graphically clear visualization of the current status of the fractures in vault's concrete. Through several passages performed on photogrammetry and geometrical rendering software, the ultimate outcome was an instrument for an immediate comprehension of the actual state of art and, so, for subsequent reasoning about its prompting causes.

The finite element model development, carried out in what can be seen as the second phase of this work, is likely the best way to gain information about the response of the tunnel structure to certain kinds of loads and stresses. As it has been underlined in the section of this thesis related to this topic, an iterative process has been followed, proceeding with hypotheses and assumptions. Therefore, from the geometry construction to the material property, ending up with constraints and loading cases, several choices and trials have been made and performed.

This dissertation aims at something that is far from being achieved in the constrained amount of time of a Master Degree's Thesis. Nonetheless, even though conclusive results have not been found, the value of this work lies in the path that it has helped tracing. In the modelling field, indeed, a trial-and-error process, composed by continuous tests and step-by-step adjustments, is commonplace and advisable. The complex nature of the situation and the number of physical entities involved, extensively explained in the general outlook provided at the beginning of this disquisition, further justifies the followed approach.

The trials developed in the conclusive part of this work are properly located in the framework just mentioned. A cantilever behavior was identified as a first

hypothesis around which initial attempts of validation of the model have been built. Since the first model, where the assumed arrangement of the constraints imposed infinite rigidity to both the closing cross-sections, traces of the assumed behavior were sought after, and, eventually, results showed that the model was misleading and generated even new doubts and questions. Then the process continued, adding, to the permanent quest of reproducing the cantilever kind of performance, the necessity of solving some arisen doubts, like the influence of the board effect. Luckily, this latter case was closed in some quick passages.

Proceeding in the effort of exploring the arisen concerns, a renewal also of the imposed movements has been implemented, switching from simple displacements applied in the center of gravity of the free-to-move section to a global pressure with a triangular increasing trend set on a delimited portion of the segment, as described in the dedicated section of this case study. This latter configuration has been unsuccessfully applied to the first model, remarking even more the deceptive nature of the assumption claiming the rigid links' network on both closing sections. Inside the discussion on the outputs of this last model's modification, a crucial mention has been given to the non-correspondence between the resulted distribution of the stresses and the reported cracks' pattern on the tunnel infrastructure.

The progression added a piece with the changing of the constraints setting, resulting in the removal of the rigid link network from the cross-section assumed to be on the unstable side. This new disposition came with the same as above global pressure charging set. All these choices were still led by the same search for the abovementioned cantilever behavior, and, specifically, came from interpretation and verification of the collected assumptions and results. The ultimate outputs of this latter model finally showed a sign of what can be seen as a cantilever behavior, both in terms of stress distribution and of deformations. However, a further verification must be searched for, especially regarding the correspondence between stresses' spreading and fractures' position.

The possible future clearly set by this work aims at constant enlargement of the amount of information to be provided to the FEM software, and at the validation of the obtained results through the monitoring data interpretative tools, like the 28th segment cracks' pattern visualization and displacement time series.

References

- » Bossi, G.; Marcato, G.; Schenato, L. “Structural Health Monitoring of a Road Tunnel Intersecting a Large and Active Landslide”, 2017, Appl. Sci., 7, 12
- » Ampezzan, D. “Three-dimensional numerical modeling of Passo della Morte (UD) Landslide for the design of risk mitigation measures”, 2017, Bologna
- » Tedesco, G. “Infrastructure maintenance and countermeasures planning in complex geological and geomorphological settings”, 2018, Bologna
- » Scuri, A. “Analisi cinematica, idrologica e proposte di intervento per il dissesto in sinistra idrografica del Rio Verde, in località Passo della Morte (UD)”, 2013, Padova
- » Marcato, G. “Valutazione della pericolosità da frana in località passo della Morte”, 2007
- » Bossi, G.; Schenato, L.; Marcato, G. “Data fusion for dissemination: web applications for the visualization of monitoring data”, 2016, Rendiconti Online della Società Geologica Italiana, vol. 39, pp. 31–34
- » Marcato, G.; Bossi, G.; Frigerio, S.; Mantovani, M.; Pasuto, A.; Schenato, L. “Relazione Finale: Convenzione protocollo n. PC/2805/CD2. Studio e monitoraggio della situazione di dissesto che interessa il versante sinistro del Tagliamento in corrispondenza del “Passo della Morte””, 2014, Padova: IRPI - Istituto di Ricerca per la Protezione Idrogeologica / CNR - Consiglio Nazionale delle Ricerche
- » Marcato, G.; Bossi, G.; Schenato, L.; Tedesco, G. “Monitoraggio della galleria di San Lorenzo in rapporto ai movimenti franosi esterni nel periodo dal 15 aprile 2020 al 15 aprile 2021 – Relazione finale”, 2021, ANAS
- » Zabuski, L.; Bossi, G.; Marcato, G. “Assessing the stability of a complex landslide through geotechnical modelling - a case study in the Carnian Alps (Italy)”, 2017, 2nd International Conference "Challenges in Geotechnical Engineering"
- » Marcato, G.; Bossi, G.; Schenato, L.; Tedesco, G. “Monitoraggio della galleria di San Lorenzo in rapporto ai movimenti franosi esterni nel periodo dal 21 novembre 2018 al 22 novembre 2019 – Relazione finale”, 2021, ANAS

- » Sinigardi, G.; Bossi, G.; Scuri, A.; Marcato, G.; Borgatti, L. “Geological and numerical models as a tool to manage landslide risk: The Passo della Morte case study (UD, Italy)”, 2015, Rend. Online Soc. Geol. Ital., 34, 46–53
- » Zabuski, L.; Bossi, G.; Marcato, G. “Influence of the Geometry Alteration of the Landslide Slope on its Stability: A Case Study in the Carnian Alps (Italy)”, 2017, De Gruyter
- » Schenato, L.; Bossi, G.; Marcato, G.; Pasuto, A. “Cumulative monitoring of strain in concrete structures with polymer optical fibers”, 2015, Rendiconti Online della Società Geologica Italiana
- » Cervi, F.; Borgatti, L.; Dreossi, G.; Marcato, G.; Michelini, M.; Stenni, B. “Isotopic features of precipitation and groundwater from the Eastern Alps of Italy: results from the Mt. Tinisa hydrogeological system”, 2017, Environmental Earth Sciences, 76
- » OpenStreetMap, [Online] Available at:
<https://www.openstreetmap.org/#map=15/46.3981/12.6906&layers=N>
- » Agisoft LLC “Agisoft Metashape User Manual: Professional Edition, Version 1.8”, 2022
- » G+D Computing Pty Limited “Straus7 Theoretical Manual – Theoretical background to the Straus/ finite element analysis system, 2004
- » Aiello, S. “L’intelligenza artificiale per caratterizzare il degrado del calcestruzzo nelle gallerie”, 2021, Torino
- » Rhinoceros3D, Rhino – Features, [Online] Available at:
<https://www.rhino3d.com/features/>